DEVELOPMENT OF A CHRONICALLY IMPLANTED MICROELECTRODE ARRAY FOR INTRANEURAL ELECTRICAL STIMULATION FOR PROSTHETIC SENSORY FEEDBACK

by

Daniel DiLorenzo

Doctor of Medicine
Harvard Medical School (1999)
Ph.D. Mechanical Engineering
Massachusetts Institute of Technology (1999)
S.M. Management of Technology
Massachusetts Institute of Technology (1999)
S.M. Electrical Engineering
Massachusetts Institute of Technology (1988)
S.B. Electrical Engineering
Massachusetts Institute of Technology (1987)

Submitted to the Harvard-MIT Division of Health Sciences and Technology
in Partial Fulfillment of the Requirements for the Degree of

Masters of Science

at the

Massachusetts Institute of Technology
June 1999

Signature of Author: _____
Daniel DiLorenzo

Signature of Thesis Supervisor: _____
David J. Edell
Principal Research Scientist
Harvard-MIT Division of Health Sciences and Technology

Accepted by: _____
Martha L. Gray, Ph.D.
J. W. Kieckhefer Associate Professor of Electrical Engineering
Co-Director, Division of Health Sciences and Technology

DEVELOPMENT OF A CHRONICALLY IMPLANTED MICROELECTRODE ARRAY FOR INTRANEURAL ELECTRICAL STIMULATION FOR PROSTHETIC SENSORY FEEDBACK

by

Daniel DiLorenzo

Submitted to the Harvard-MIT Division of Health Sciences and Technology
in Partial Fulfillment of the Requirements for the Degree of
Master of Science

ABSTRACT

The functionality of prosthetic limbs is restricted by the limited availability of sensory feedback. This research aims to develop a technology to allow the presentation of sensory information directly to the sensory afferent neurons of the transected peripheral nerve in the stump of the amputee. Intraneural implants of several designs were developed and implanted in rabbit animal models and monitored for chronic functionality evaluated using both neurophysiological and behavioral tests. Animal studies have demonstrated single channel implant functionality of up to 129 days. The relative merit of the designs is assessed, and future directions for implant design and behavioral testing are suggested.

Thesis Supervisor: David J. Edell

Title: Principal Research Scientist

Acknowledgments

I am dedicating this thesis to my parents, Dr. Henry and Marian DiLorenzo, who have been an limitless source of encouragement throughout all of my pursuits. I am indebted to the guidance and support I received from my advisor David J. Edell, who possesses an immense wealth of knowledge of all aspects of neuroelectric interface development. I would like to thank Ron R. Riso for his invaluable help in developing the behavioral animal model. I am thankful to Lisa P. Devaney for her tireless assistance in fabricating implants and in conducting experiments. Bruce C. Larson is owed credit for his expertise in developing some of the instrumentation used in these experiments. The Brockton-West Roxbury VA Medical Center provided essential labspace, histology and surgery resources for conducting the experiments. Lincoln Laboratories provided cleanroom facilities for fabricating the implants

DEVELOPMENT OF A CHRONICALLY IMPLANTED MICROELECTRODE ARRAY FOR INTRANEURAL ELECTRICAL STIMULATION FOR PROSTHETIC SENSORY FEEDBACK

Daniel J. DiLorenzo

Table of Contents

DEVELOPMENT OF A CHRONICALLY IMPLANTED MICROELECTRODE ARRAY FOR INTRANEURAL ELECTRICAL STIMULATION FOR PROSTHETIC SENSORY FEEDBACK

Daniel J. DiLorenzo

Table of Figures

DEVELOPMENT OF A CHRONICALLY IMPLANTED MICROELECTRODE ARRAY FOR INTRANEURAL ELECTRICAL STIMULATION FOR PROSTHETIC SENSORY FEEDBACK

Daniel J. DiLorenzo

Table of Tables

INTRODUCTION

Motivation

A major factor restricting the functionality of prosthetic limbs is the limited availability of sensory feedback. Cable-driven prostheses inherently provide force and position feedback to the driving muscle group; however, this is usually limited to single channel joint information. Powered prostheses offer the possibility of increased dexterity; however, extraction of motor and provision of sensory information becomes the limiting factor. Current technology incorporates electromyographic (EMG) signal processing to extract motor commands from remaining stump musculature. Limited enhancement of prosthesis functionality has been reported with sensory feedback configurations using surface electrical and vibrotactile stimulation. Prior work has demonstrated the functionality of single channel implanted interfaces for chronic sensory feedback [1-3]. Chronic interfaces for multichannel *recording* have been developed [4, 5]. This project aims to develop a technology capable of providing multichannel sensory feedback via an implanted microelectrode *stimulating* array.

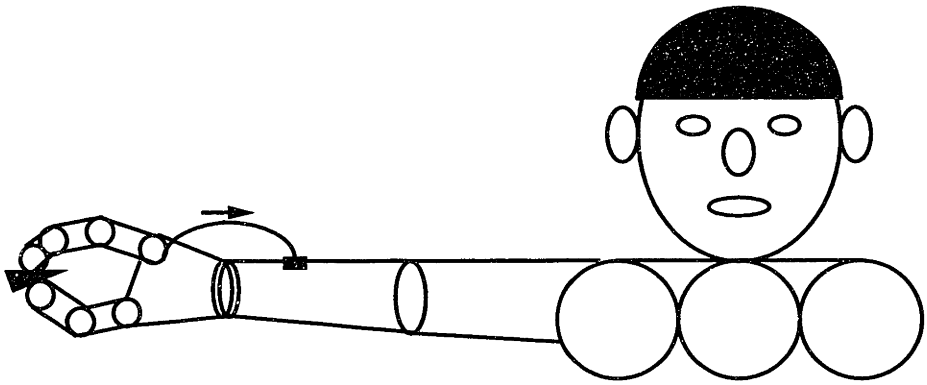

Figure 1: Sensory Feedback from Instrumented Prosthesis

Overview of Sensory Feedback Systems for Limb Prostheses

Surface Sensory Feedback Interfaces

Electrocutaneous nerve stimulation was discovered in 1745 by von Kleist who described a shock from an electrostatically charged capacitor [6]. Studies published by von Frey in 1915 [7] and Adrian in 1919 [8] demonstrated the spectrum of sensations elicited by electrocutaneous stimulation, ranging from vibration to prickling pain and stinging pain. The purpose of most of the hundreds of subsequent publications fall into one of three categories: studies of

the nervous system and its pathology and pharmacology, studies of the relation of stimulus parameters to perceived sensation, and the transmission of information to the organism including prosthesis sensory feedback.

In 1966, Beeker described an artificial hand with electrocutaneous feedback of thumb contact pressure. Initial results, although qualitative, were positive [9]. In 1977, Schmidl reported that electrocutaneous sensory feedback of grip strength improved control of an experimental hand. He found electrocutaneous feedback to be less susceptible to adaptation than vibrotactile feedback [10]. In 1979, Shannon showed that electrocutaneous feedback on the skin above the median nerve is used to encode gripping force in a myoelectrically-controlled prosthesis, patients reported an improved level of confidence when using the prosthesis [11]. No objective measures of performance were made, however. Earlier implementations of electrocutaneous stimulation interfered with recording of myoelectric control signals. This has since been overcome by strategies such as isolating the recording and stimulating grounds [12] and using a sample-hold in the control circuit [13]. Comparisons of the major feedback coding schemes have shown that multiple electrode displays using spatial modulation perform better than amplitude (AM) or frequency modulation (FM) codes [14]. This represents but a sampling of the most relevant literature; more comprehensive coverage is given in several excellent reviews [15-18].

Clinical application of electrocutaneous displays is limited primarily by uncomfortable sensations. This may be alleviated by development of stimulation parameters that allow differential excitation of afferent fibers, particularly those that minimize C fiber excitation. Present electrodes and waveforms may cause skin irritation after several hours of stimulation. Difficulty in achieving uniform skin contact further complicates skin irritation.

Vibrotactile feedback has been shown to provide information transmission capabilities essentially identical to electrocutaneous systems. Its major advantages are universal psychological acceptance among patients and lack of stimulus artifact which might interfere with EMG recording. Its disadvantages include larger size, greater power consumption, and difficulty in implementing such a system in a practical and cosmetic fashion [19].

Implanted Sensory Feedback Interfaces

Scarce research is published in the area of prosthetic sensory feedback via implanted stimulating electrodes. The only published work found in implanted sensory feedback from prostheses is that conducted by Clippinger [1].

In 1974, Clippinger implanted a sensory feedback system incorporating an electrode pair to stimulate the median nerve. He provided a frequency modulated signal which transmitted gripping force at the terminal hook. Patients were able to perceive grip force as well as object consistency [1]. In 1977, Clippinger reported a system using implanted electrodes to provide afferent sensory feedback for upper extremity amputees [2]. The same year, he reported

that postoperative stimulation of the sciatic nerve by a lower-extremity prosthesis offered the additional benefit of postoperative pain reduction [3]. In 1982, he reported six year success in a lower-extremity amputee using sciatic nerve stimulation to transmit heel strike force and leg structure bending moment on a single channel. No further work on implanted sensory feedback prostheses is published by Clippinger.

In 1985, Lovely published a technical note in which he described a system employing a bi-directional RF link to communicate with an implanted stimulator and recorder. His application was the recording of myoelectric signals to control a prosthetic hand while providing sensory feedback [20]. No animal or human trials are reported in this or subsequent publications.

Chronic stimulating electrodes have been implanted since 1965 to alleviate pain [21] [22] [23].

Background on Nerve Regeneration and Chronic Interfaces

Peripheral Nerve Regeneration through Silicone Cuffs

Considerable work has been done in the development of nerve regeneration tubes for enhancement of regeneration by injured peripheral nerves. Extensive evaluation of the regeneration of nerve through silicone and a variety of other materials has been conducted [24]. The influence of the length of the gap between the proximal and distal nerve stumps [25] as well as the presence of the distal stump [26] have been investigated. These studies demonstrate diminished or absent long term regeneration in the absence of a distal nerve stump. Thus, one of the first obstacles to the development of a chronic neuroelectric interface for prosthetic sensory feedback is the demonstration that a chronic interface can be maintained in the absence of a distal stump.

Chronic Viability of Transected Peripheral Sensory Axons

Prior studies have investigated the chronic viability of transected peripheral sensory axons. Histological studies have shown that following peripheral nerve transection, all axons undergo atrophy; and this is only reversed if the fibers regenerate and establish functional connections [27, 28]. If functional connection is reestablished, fiber diameters increase and may approach their original sizes [29-31].

Animal studies indicate that in the early phases (0 to 45 days) following peripheral nerve transection, sensory fiber atrophy is not significantly different from that of motor fibers; however, after 145 to 245 days, while motor fibers have atrophied according to an exponential decay to 35% of control values, sensory

fibers have decayed to virtually zero [32]. Despite these findings, successful chronic stimulation of sensory axons has been reported [1].

Chronic Peripheral Neural Interfaces

The first successful chronic implantation of an electrode designed to interface with regenerating axons was described by Marks in 1969 [33]. This electrode was implanted in the peripheral nerve of a frog and consisted of a thin disk with perforations through which axons regenerated. The first successful recording from a chronically implanted regeneration electrode was reported by Mannard *et al.* in 1974 [34]. Subsequent successful implantation of mammalian nerves had been hampered by increased propensity for fibrosis [35, 36]. Fibrosis has been attributed to disorganized regeneration of axons [37].

Edell first described the successful chronic implantation of a silicon microelectrode array for neural recording [4, 38, 39]. Edell reasoned that disorganized regeneration was due to obstruction of the regeneration path by electrode materials, and he sought to minimize this obstruction. His design consisted of a silicon substrate which was chemically etched anisotropically to produce rectangular slots traversing the Silicon. These rectangular slots measuring 160 microns in width provide paths through which transected axons may regenerate. The silicon strips dividing the slots were far narrower than the slots, measuring 40 microns in width, minimizing the cross-sectional area of, and thus the obstruction to regeneration posed by, the implant. This strip width was chosen to provide sufficient space for multiple conductive paths and incorporation of active electronics. In the process of regenerating, these axons are positioned in close proximity to the electrode surfaces lining the rectangular holes, facilitating electrical recording from the axons.

Objectives

The performance of prosthetic limbs is severely hampered by absence of sensory feedback information. The success of chronic recording from peripheral nerves using macroelectrodes as well as microelectrodes coupled with early reports of successful chronic stimulation using implanted macroelectrodes, the development of a microelectrode array for chronic stimulation appears to be a potentially fruitful area of technology development and investigation.

The first objective is the design of a multichannel microelectrode interface fro chronic implantation which remains functional within the harsh environment of the body. These requirements include robustness to (1) physical movement and fatigue, (2) electrolytes including saline, (3) immunological responses including fibrosis and encapsulation.

The second objective is the demonstration of the chronic viability of sensory axons following nerve transection and in the absence of a distal nerve stump or sensory organs. As discussed above, prior studies have suggested that without distal innervation of sensory organs, afferent fibers will atrophy.

The third objective is the characterization of the long-term in-vivo electrode impedance. This allows quantification and assessment of the degree of encapsulation and degradation, if any, of the electrode surfaces. This measure also allows determination of the stimulation currents required to achieve neuronal activation.

The fourth objective is the determination of sensory perception thresholds. This represents the minimum amount of electrical stimulation current required to elicit a perception. This stimulation threshold is to be minimized and must be sufficiently low to avoid damage to the neural tissue and the electrode surface.

Animal Model Development

Overview

Characterization of an implanted stimulating electrode array required development of an animal model in which implant functionality, assessed both neurophysiologically and behaviorally, and nerve histology could be evaluated. New Zealand white rabbits were selected because of their size and ease of handling. The sciatic nerve was used because of its accessibility and mobility and the minimal functional deficit transection imparts to the animal. In the 4 to 5 kilogram rabbits used, a length of sciatic nerve, ranging approximately from 6 to 8 centimeters, can be dissected and mobilized from the fascia between the hip abductors and the femur.

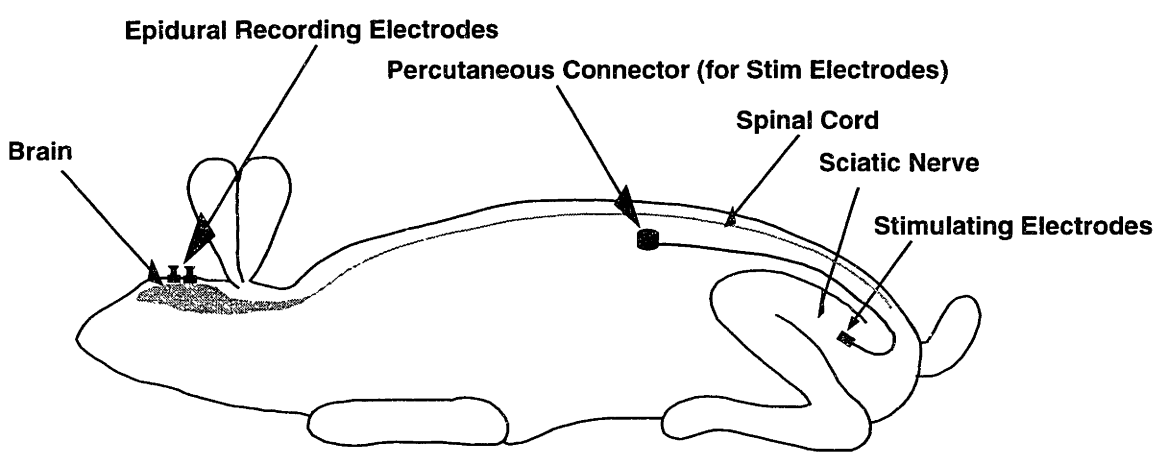

Figure 2: Animal Model Stimulating and Recording Electrode Configuration

Several stimulating electrode array designs have been investigated using the rabbit animal model depicted in Figure 2. In this model, the left sciatic nerve is transected, and the proximal stump is drawn into a silicone cuff containing the electrode array. The transection is made at the level of the distal femur, and the sciatic nerve is positioned to loop back upon itself in the mid femur region and travel proximally to the implant mounted by the head of the femur. This location of the implant minimizes movement, thereby reducing mechanical fatigue of the Platinum-Iridium (Pt/Ir) wires used in its construction.

Neurophysiological monitoring of the electrical stimulus is accomplished by four epidural cortical electrodes implanted over the somatosensory cortex. Two are located above each of the ipsilateral and contralateral somatosensory cortex corresponding to the hind paw. This location was found experimentally to be 3 mm lateral to and 1 mm posterior to the bregma; this is consistent with somatosensory mapping reported previously in the literature [40].

Figure 3 is a sketch of the somatosensory cortical representation of the lower limb and surrounding eloquent areas. The cortical representation of the hind limb of the rabbit is small, measuring approximately 0.5 cm in diameter [40].

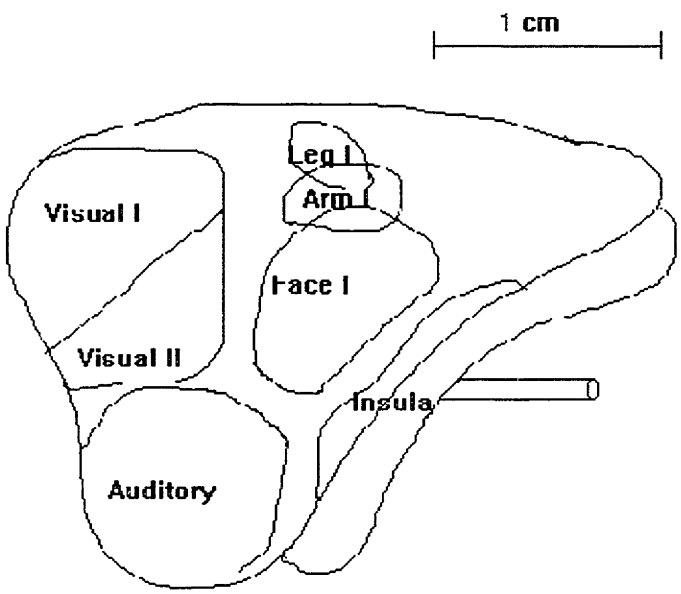

Rabbit Somatosensory, Visual, and Auditory Cortical Areas

Figure 3: Sketch of Somatosensory Cortical Mapping (adapted from Woolsey, 1946)

A total of 28 rabbits were evaluated, including 19 chronic stimulating implants, 6 nerve regeneration tube array implants, and 3 acute cortical mapping experiments (see Table 1). Of the 19 chronic stimulating implants, 6 were evaluated using a dual nerve cuff implant

Rabbit	Implantation Date	Study	Stim/Record Configuration					
			Stimulating Array				Rec. Electr	Animal
			Electrodes	Placement	Length	Cuff		Model
AA	Jun-93	chronic implant	[axial w ire]			Silastic	nerve cuff	dual cuff
AB	Jun-93	chronic implant	[axial w ire]			Silastic	nerve cuff	dual cuff
AC	12/17/94	chronic implant	axial w ire	hexagonal array	[1 mm exposed tip]	Silastic	nerve cuff	dual cuff
AD	Jan-94	chronic implant	axial w ire	hexagonal array	[1 mm exposed tip]	Silastic	nerve cuff	dual cuff
AE	Jan-94	chronic implant	axial w ire	hexagonal array	[1 mm exposed tip]	Silastic	nerve cuff	dual cuff
AF	Jan-94	chronic implant	axial w ire	hexagonal array	[1 mm exposed tip]	Silastic	nerve cuff	dual cuff
AG	4/1/94	chronic implant	axial w ire	hexagonal array	[1 mm exposed tip]	Silastic	epidural	cuff & epidural
AH		chronic implant	axial w ire	hexagonal array	[1 mm exposed tip]	Silastic	epidural	cuff & epidural
AI		chronic implant	axial w ire	hexagonal array	[1 mm exposed tip]	Silastic	epidural	cuff & epidural
AJ	6/24/94	ACUTE cort map	hook pair	suspended nerve	5-10 mm spacing	none	epidural array	acute
AK	6/24/94	chronic implant	axial w ire	hexagonal array	[1 mm exposed tip]	Silastic	epidural	cuff & epidural
AL	7/1/94	chronic implant	axial w ire	hexagonal array	[1 mm exposed tip]	Silastic	epidural	cuff & epidural
AM	7/8/94	chronic implant	axial w ire	hexagonal array	[1 mm exposed tip]	Silastic	epidural	cuff & epidural
AN	8/19/94	ACUTE cort map	hook pair	suspended nerve	5-10 mm spacing	none	epidural array	acute
AO	8/26/94	chronic implant	regen tube	7 silastic tubes	[5 mm tubes]	Silastic	epidural	cuff & epidural
AP	9/12/94	chronic implant	regen tube	7 silastic tubes	[5 mm tubes]	Silastic	epidural	cuff & epidural
AQ		[chronic implant]						[cuff & epidural]
AR	10/14/94	nerve regenerat	none	12 silastic 0.012" i	10 mm tubes	Silastic		no electrodes
AS	10/14/94	nerve regenerat	none	12 silastic 0.012" I	2 mm tubes	Silastic		no electrodes
AT	10/26/94	nerve regenerat	none	12 silastic 0.012" I	1 mm tubes	Silastic		no electrodes
AU	10/26/94	nerve regenerat	none	12 silastic 0.012" I	5 mm tubes	Silastic		no electrodes
AV	10/26/94	nerve regenerat	none	12 silastic 0.012" I	10 mm tubes	Silastic		no electrodes
AW	11/18/94	nerve regenerat	none	12 cast NuSil 621C	[4] mm tubes	NuSil 4211 w	strain relief	no electrodes
AX	11/18/94	ACUTE cort map	hook pair	suspended nerve	5-10 mm spacing		epidural array	acute
AY	1/9/95	chronic implant	hybrid				epidural	cuff & epidural
AZ	2/17/95	open quartz tube	open-ended Quartz tube w axial electrodes					
BA	3/28/95	not implanted	none				none	(glaucoma)
BB	3/28/95	chronic implant	Quartz tube w ith axial w ire array					cuff only
BC	4/28/95	chronic implant	Silicone cuff w ith 3 epineural ring electrodes					cuff only

Table 1: Rabbit and Implant Configuration Summary

Functional Assessment of Implant

Two evaluation methodologies were employed to monitor and assess functionality of the implants: neurophysiological and behavioral. Neurophysiological monitoring is well characterized in the literature, but it's sensitivity is limited by a low signal to noise ratio. Behavioral conditioning offers the potential to achieve greater sensitivity; however, it is dependent upon cooperation of the animal.

Neurophysiological Monitoring Techniques

Two methods for neurophysiological monitoring were explored. Initially, epineural compound action potentials were recorded to monitor implant functionality. Evidence suggesting compromise to neural regeneration due to implantation of the second and proximal recording electrode cuff prompted a change to monitoring of somatosensory evoked potentials.

Epineural Compound Action Potential Recording

Six rabbits, AA through AF, were implanted with dual cuffs; the implant configuration within the rabbit is depicted in Figure 4, and the relationship of the two cuffs on the sciatic nerve is shown in Figure 5. The stimulating electrode array consisting of 10 to 12 axially oriented stimulating Pt/Ir wire electrodes was placed at the distal end of the transected proximal nerve stump (see Figure 6). The recording electrode array consisting of three epineural ring electrodes was placed several centimeters proximal to the stimulating electrode array (see Figure 7).

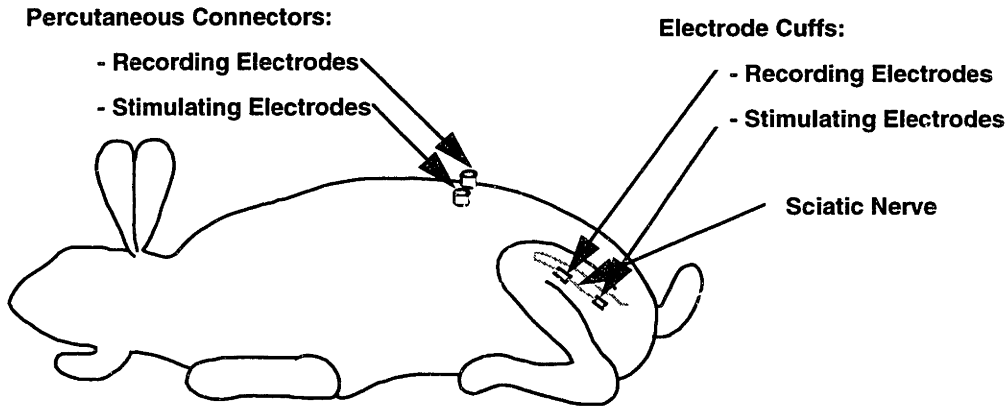

Figure 4: Stimulating/Recording Dual Nerve Cuff Implant Model

The animal model is depicted in Figure 4. During implantation, The left sciatic nerve of a New Zealand white rabbits is transected just proximal to its trifurcation into the peroneal, tibial, and cutaneous branches at the distal end of the femur. The proximal end is inserted into a recording electrode cuff which is advanced to approximately 8 cm proximal to the transection. This same proximal nerve stump is subsequently inserted into an array of axially oriented stimulating electrodes. The stimulating array consists of 10-12 wire electrodes electrochemically etched to increase surface roughness and hence surface area. The recording electrode cuff consists of three epineural wire loops oriented along the circumference of the nerve.

Electrical cables from each electrode cuff course in the subcutaneous plane to the lower thoracic paraspinal region of the back, where they connect to percutaneous plugs. Each percutaneous plug is sutured to the superficial facial layer. A die is used to create a circular perforation through the skin. The plug is pressed through this opening, resulting in a snug fit between the skin and circumference of the percutaneous plug. The nerve and cuffs are oriented such that the sciatic nerve courses distally and then loops back proximally before passing through the recording electrode cuff and then the stimulating electrode cuff. This free-floating loop minimizes tension and strain exerted by the implants on the nerve.

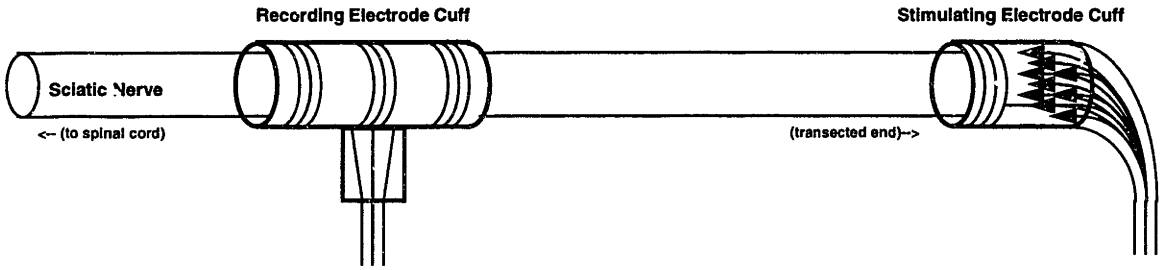

Figure 5: Stimulating/Recording Dual Nerve Cuff Configuration

The stimulating and recording electrode configuration is depicted in Figure 5. The recording electrode cuff is placed around the distal end of the proximal nerve stump. The nerve is then drawn through the implant, such that the recording electrode cuff is situated several centimeters proximal to the transected nerve end. Then, the stimulating electrode cuff is sutured to the distal end of the proximal transected nerve stump. Each of the two cuffs is sutured to the deep fascia and muscles overlying the femur.

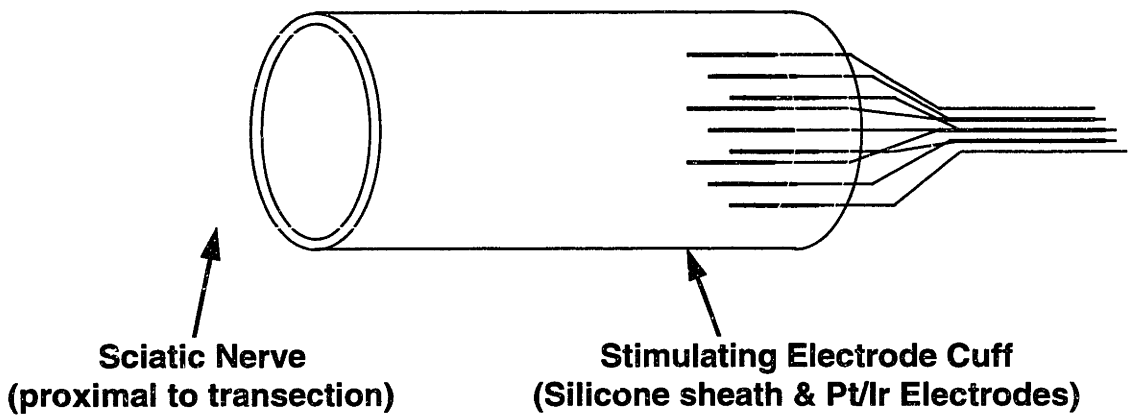

Figure 6: Axially-Oriented Pt/Ir Wire Electrode Stimulating Array

The stimulating electrode cuff is shown in Figure 6. The cylindrical body in the center is fabricated from silicone. Designs comprised from each of prefabricated silicone tube and cast silicone were produced. An array of axially oriented platinum-iridium (Pt/Ir) wire electrodes are shown on the right. The distal portion of the proximal nerve stump is shown on the left, inserted into the nerve cuff. Prior to insertion, the distal 1-2 mm of epineurium are removed, exposing a bundle of individual fascicles. This is inserted into the nerve cuff such that the nerve tip is adjacent to the tips of the electrodes. After insertion, three sutures are placed between the proximal end of the nerve cuff and the epineurium.

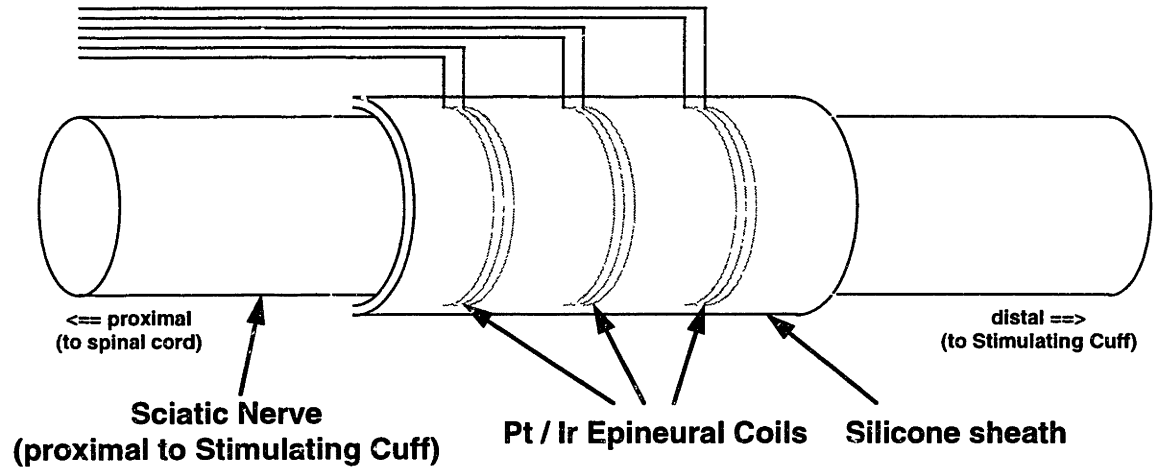

Figure 7: Triple Epineural Ring Recording Electrode Array

The recording electrode cuff is depicted in Figure 7. The body of the recording electrode cuff is constructed from silicone tube. During fabrication, the deinsulated portions of three platinum-iridium (Pt/Ir) wires are wrapped around a dowel. Uncured silicone is applied to stabilize these three wire coils, and an outer cylindrical silicone tube, in which a longitudinal slit has previously been made, is placed around the coils. Uncured silicone is used to seal the longitudinal slit. The Pt/Ir wires have a conductor diameter of 2 mils with an outer insulation diameter of 3 mils. The Pt/Ir wires are fed through a larger silicone tube which functions as an outer protective and insulation layer. The Pt/Ir wires are then soldered to the contacts of the percutaneous plug, and all exposed conductive surfaces are covered with uncured silicone. The assembly is then cured according to one of several curing schedules, including either of room or elevated temperature cures.

In measuring the compound action potential (CAP), the two outer of the three electrodes were connected in parallel, and differential mode amplification of the signal from the central electrode relative to the outer electrode pair was performed. This technique serves to minimize the magnitude of the electromyogram (EMG) and stimulus artifacts and increase signal to noise ratio. Firm apposition of the nerve cuff to the epineurium also serves to minimize the volume of intervening conductive fluid, and maximize the resistance to current arising from EMG and stimulus artifact sources.

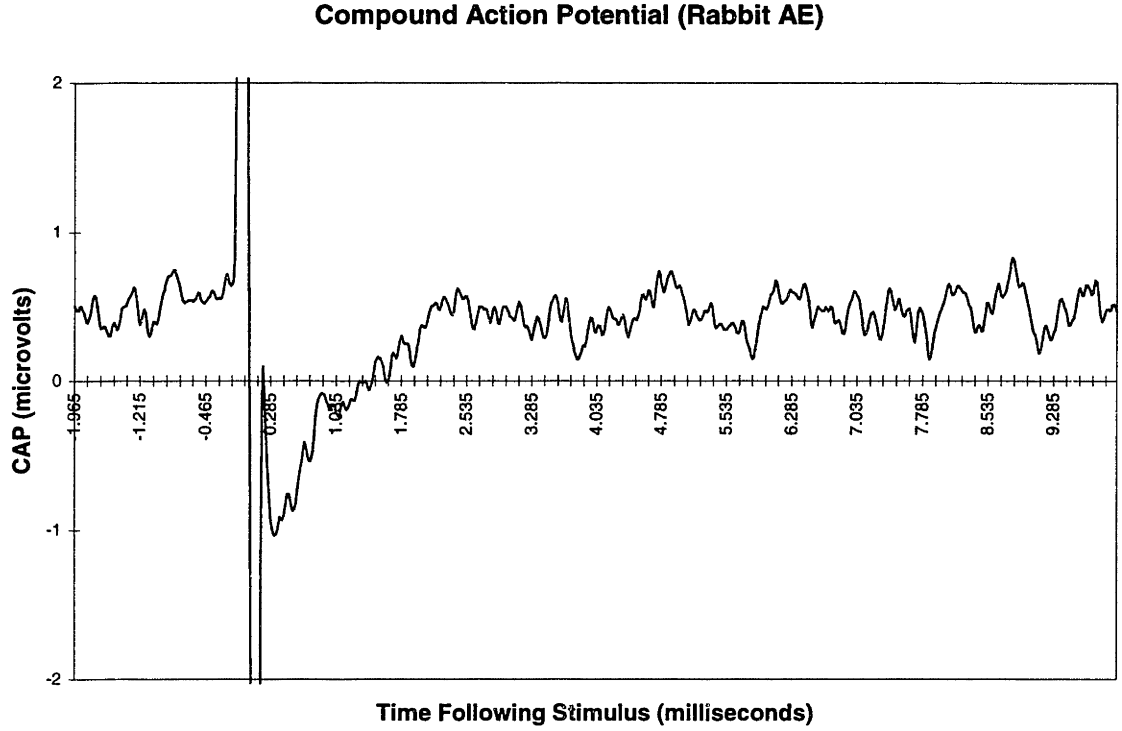

Figure 8: Compound Action Potential from Triple Epineural Ring Recording Electrode Array

A representative presumed compound action potential recorded from this electrode configuration is shown in Figure 8. The stimulus artifact is evident at time 0, followed shortly by the compound action potential with a peak at 0.33 milliseconds. For a stimulating to recording electrode cuff spacing of approximately 8 cm, this would correspond to a conduction velocity of 242 m/s, which is much higher than the typical 100 m/s that would be expected. This is suggestive of stimulation of nerve tissue proximal to the stimulating nerve electrode cuff. This would be consistent with absence of viable nerve within the stimulating electrode cuff, as was found subsequently upon explanation. This experiment was repeated with stimulus waveforms of opposite polarity, and compound action potentials of the unchanged polarity were recorded, providing evidence that the signal was neural in origin rather than an artifact arising from the stimulus.

Although some success was had with this configuration, the dual trauma to the peripheral nerve induced by the electrode cuff pair appears to have substantially impaired axonal regeneration in several of the animals. Several histological specimens revealed no axonal regeneration into the distal cuff. For this reason, the site of recording was changed from the peripheral nerve to the somatosensory cortex. Additionally, strain reliefs were designed into the stimulating electrode array cuff to further minimize mechanical trauma to the implanted nerve.

Epidural Somatosensory Cortical Recording

Neurophysiological monitoring consisted of recording of cortical evoked potentials from electrodes placed above the somatosensory cortex contralateral to the stimulating electrode array. Evoked potential monitoring is an established technique employed to monitor sensory stimuli; however, its sensitivity is constrained by two major factors. Physiological cortical noise substantially limits the signal to noise ratio of the recorded potential, and activation of large pcpulations of sensory afferents is required to generate a detectable cortical response. A low noise differential mode isolated recording amplifier was designed and built to better enable signal detection. Signal averaging is emplcyed to improve the signal to noise ratio.

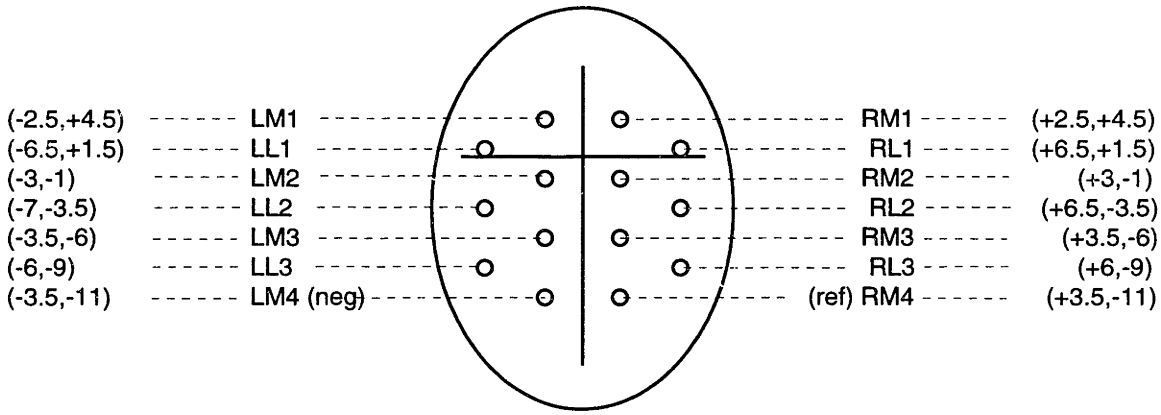

Figure 9: Acute Epidural Somatosensory Mapping: Cortical Electrode Placement

Optimal placement of somatosensory recording electrodes was determined by review of the literature [41] (see Figure 3)and acute cortical mapping experiments. Stainless steel epidural posts with an intracalvaral portion consisting of 5 turns of 4-40 thread and a smooth polyimide insulated transcutaneous shaft were used for the recordings. Figure 9 depicts the approximately hexagonal grid of electrodes were secured to the calvarum using bone cement to mechanically augment the threaded turns and supplement the polyimide electrical insulation coating on the posts. Labels for each electrode are shown to the side of the diagram of the head, and the coordinates relative to the bregma are given at the lateral edge of the figure.

In the experiment which gave rise to the data shown in Figure 10, the left sciatic nerve was suspended on silver hook electrodes and stimulated using each of 350 and 450 microamps (pulse width 100 microseconds, charge balanced), and the distal tibial and peroneal branches were each separately stimulated at 450 microamps (pulse width 100 microseconds, charge balanced). These configurations are noted in the legend by "sci-350", "sci-450", "tib-450", and "per-450", respectively. Note the greater activity over the contralateral (right)

somatosensory cortex in response to sciatic nerve stimulation. These voltages recorded over the contralateral cortex (electrodes RM2, RM3, RL1, and RL2) are similar, indicating either a broad region of activity encompassing these electrodes or a region approximately equidistant from these electrodes. In contrast, and consistent with known neurophysiology, the activity recorded over the ipsilateral (right) cortex is less in response to sciatic nerve stimulation. The right cortical activity elicited by tibial nerve stimulation is higher than what might be expected. The large peak observed in electrode LM2 may be due to placement of that electrode precisely above the ipsilateral cortical area representing the region subserved by the tibial nerve. Perhaps none of the positions of the contralateral electrodes was so closely aligned with the corresponding contralateral cortical region. This data was obtained from a single acute experiment; it was designed to and did verify somatosensory mapping data found in the literature. A larger number of animals would certainly be required to generate a statistically significant array of electrically evoked potential cortical mapping amplitudes.

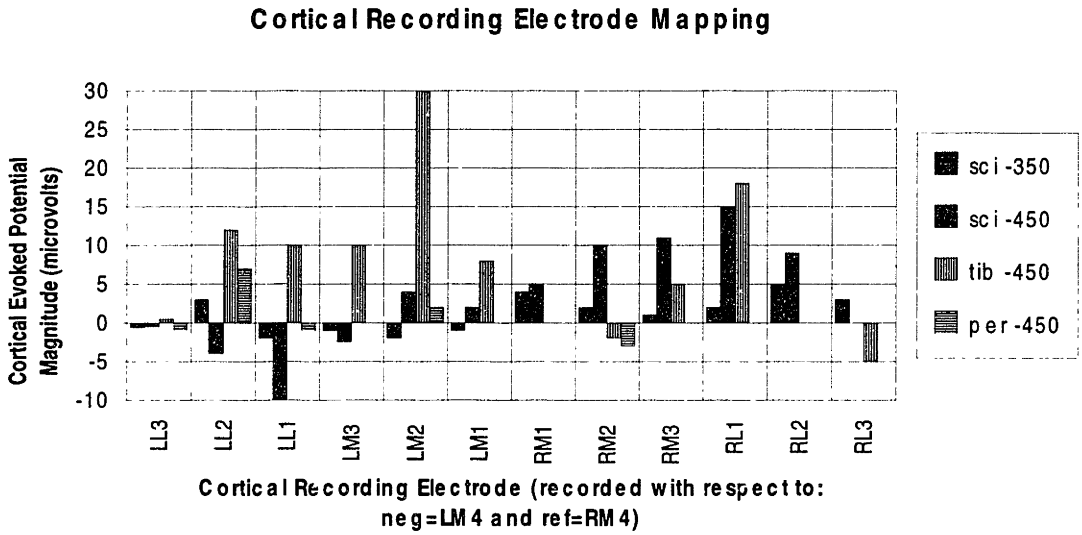

Figure 10: Acute Somatosensory Evoked Potential Mapping Experiment: Amplitudes

The acute somatosensory electrically evoked potential signal amplitudes for each electrode are shown in Figure 10. The largest amplitude evoked potential was recorded from the contralateral electrode located 3 mm and 1 mm posterior to the bregma. The results were in agreement with rabbit hind limb somatosensory representation [40] [42].

Behavioral Conditioning: Eye-Blink Reflex

Behavioral monitoring was used to supplement neurophysiological monitoring. A classical conditioning technique was used to train a rabbit to associate a conditioned stimulus with an unconditioned stimulus-response reflex. In this case, the unconditioned stimulus is an airpuff delivered to the left eye, and this elicits the unconditioned eye-blink response. An electrical stimulus applied to the implant 300 milliseconds before the airpuff is produced comprises the conditioned stimulus. An infrared (IR) emitter-detector pair is used to measure the infrared (IR) reflectance of the eye (see Figure 11).

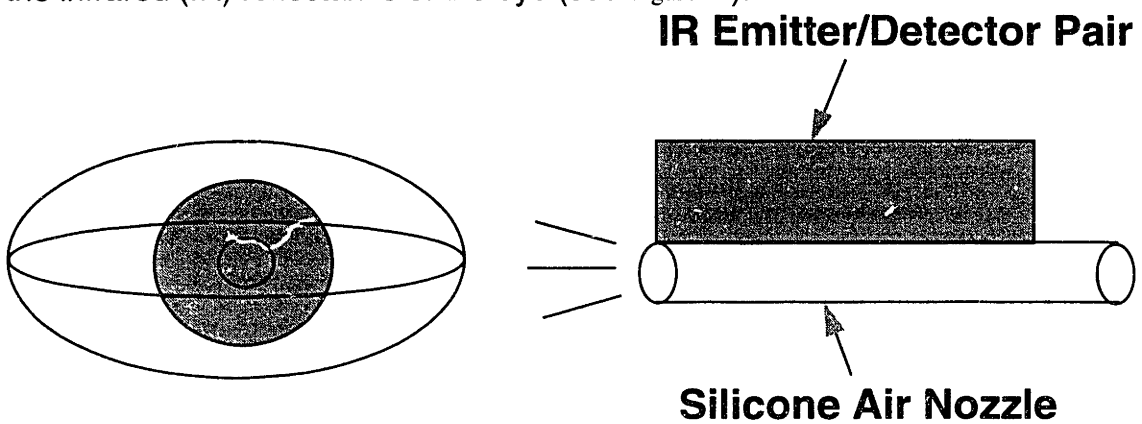

Figure 11: Eye-Blink Behavioral Conditioning Configuration

With training, the conditioned electrical stimulus becomes associated with the airpuff such that delivery of the electrical stimulus alone (in the absence of the airpuff) elicited an eye-blink. Initially, the eye-blink follows the airpuff onset by approximately 50 milliseconds. As the learning progresses, the eye-blink response is observed to advance in time. These time waveforms are shown in Figure 12. This method facilitates evaluation of animal perception of the delivered stimulus. Because the perception threshold is believed to be much lower than the evoked potential detection threshold, the behavioral conditioning offers the possibility of much more sensitive assessment of implant functionality.

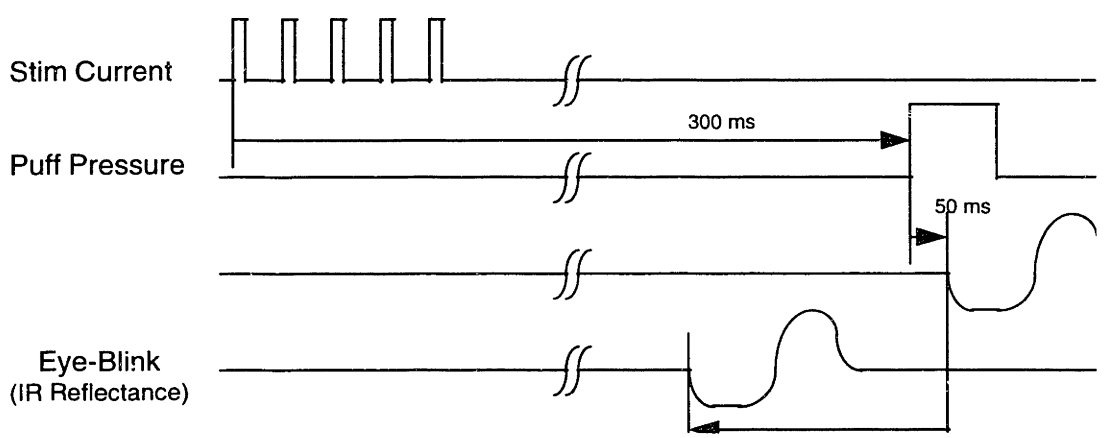

Figure 12: Eye-Blink Behavioral Conditioning Timing Sequence

Implantation Procedure

Preoperative preparation consisted of induction of anesthesia with intramuscular Ketamine and Xylazine prior to shaving the back, left leg, and head. Betadine scrub was applied and rinsed to cleanse and disinfect the operative regions. This was followed by application of betadine to the operative regions. The animal was then positioned lying with its head upright on the table, forelimbs symmetrically placed lateral to the head, and lower limbs and lower back positioned resting on the right side. Electrocardiogram (EKG) leads were placed and the animal was draped with sterile surgical drapes. The head was placed in a small animal anesthesia cone, and anesthesia was maintained with constant flow Isoflurane and air mixture. Anesthesia depth was monitored intraoperatively via heart rate monitoring from EKG leads.

Sciatic Nerve Stimulating Array Implantation

An incision was made beginning proximal to the head of the femur and was continued distally to the just proximal to the distal end of the femur. Monopolar electrocautery was used to control bleeding. Subcutaneous tissues were dissected to reveal the quadriceps and hamstrings. Dissection was continued to isolate the sciatic nerve. No electrocautery was used once the sciatic nerve was reached or within 1-2 centimeters as it was being approached.

The sciatic nerve was dissected free for its length adjacent to the femur down to the point immediately proximal to its trifurcation into tibial, peroneal, and cutaneous branches, with care taken not to disrupt its blood supply. Two to three drops of lidocaine were applied to the intended site of transection. After waiting approximately 30 seconds for the lidocaine to diffuse into the nerve, the nerve was transected. The implantation of the stimulating and recording electrode cuffs are described above.

During a postoperative recovery phase lasting from 3 to 5 weeks, the axons from the transected proximal nerve stump regenerate through the ample space within between the wire electrodes. In the first several designs, regeneration continued up to a level 1-2 mm proximal to the distal end of the closed end of the nerve cuff, leaving a 1-2 mm long "plasma" zone. It was postulated that accumulation of neural regeneration inhibitory factors was preventing regeneration of the axons to the distal end of the cuff. To overcome this, a ring of "regeneration ports" lining the circumference of the distal end of the electrode cuff were included in subsequent designs. As anticipated, axons regenerated through these ports, and in many cases, a neuroma was formed outside of and distal to the nerve cuff as these regenerating threads reconverged.

Epidural Somatosensory Cortical Recording Electrode Implantation

Following implantation of the stimulating electrode cuff and recording electrode cuff, if included, epidural electrodes were placed overlying the contralateral somatosensory cortex. These cortical recording electrode posts were machined from 4-40 titanium threaded rod and measured approximately 8 mm in length. The base portion consisted of 4 turns of threaded rod. Above this region, the rod was machined to approximately 1 mm in diameter. A circumferential notch was placed 1 mm from the top of the post; to facilitate robust grasping by recording electrode alligator clips. A flat was machined into the side of the threads, to allow locking of rotation with bone cement. Polyimide was applied to the shaft of the post up to just below the level of the notch, providing electrical insulation from the skin.

Holes were drilled in the calvarum, with care taken not to disrupt the dura. The bone was tapped manually with a sterile 4-40 tap drill. The posts were screwed into the threaded holes. Bone cement was applied into the flat on the threads to lock post rotation and surrounding the post to provide mechanical support. Using a #11 scalpel blade, holes were made in the skin corresponding to the post locations, and the skin was drawn over the recording electrode posts and sutured together at the midline.

Immediately postoperatively, the stimulating electrode impedances were tested and evoked potential recordings were made. The impedances verified continuity of solder connections and electrical cables. Stimulation thresholds were determined to verify intact placement of the nerve within the stimulating electrode cuff.

Discussion of and Future Recommendations for Animal Model

The epidural somatosensory evoked potential monitoring generated consistent data and the hardware proved to be mechanically robust in most cases. Occasional loosening of the electrode posts did occur; however, inclusion of the flat on the threads reduced the incidence of this. The length was chosen to be as short as possible while reliably allowing extension above the top of the skin. With shorter lengths come reduced torque applied to the base by contact of the animal's head with objects in the environment, i.e. metal cage. Extension above the skin was required to minimize effects of EMG and other noise signals carried by the skin and to minimize the risk of infection posed by accumulated material in the electrode post notch which could otherwise come into prolonged contact with the skin.

Dual nerve cuffs for stimulating and recording proved to be ineffective, with occasional but not consistent recordings of compound action potentials.

Eye blink conditioning proved consistent in assessing implant functionality. Stimulation thresholds calculated from the behavioral testing were similar to those determined neurophysiologically. Further anticipated improvements include implementation of automated variation of stimulation currents in a staircase fashion. Additionally, hardware has been designed and built for testing of both eyes for dual-channel behavioral testing.

Chronic Stimulating Neuroelectric Interface: Design

Design Objectives and Constraints

Development of a chronic neuroelectric interface involves satisfaction of three primary objectives and a fourth for multichannel designs: (1) regeneration of axons in close proximity to electrode surfaces, (2) mechanical robustness of implant and connecting leads, (3) minimization of stimulation current threshold, and (4) maximization of stimulation specificity (or reduction of crosstalk) in a multichannel design .

As postulated by Edell [4], successful neural regeneration is dependent upon minimization of mechanical obstruction. The wire array design described below provides negligible cross-sectional resistance to axonal regeneration and produced reliable interfacing. Stimulation current density decays with an approximately $1/r^2$ distribution; as such crosstalk is difficult to avoid with this design. A regeneration tube design was developed and tested to provide stimulation of specific neuronal subpopulations, i.e. minimize crosstalk, and to substantially reduce stimulation current thresholds. In immediate postoperative testing, the regeneration tube design did produce remarkably lower stimulation thresholds (3 microamps); however, further research remains to achieve satisfactory chronic regeneration through the narrow regeneration tubes.

Implant Designs Evaluated

Twenty eight devices have been built and tested in animal models. Of these, six have been passive regeneration tubes implanted as part of a pilot study conducted to assess peripheral nerve regeneration capability through tubes of small diameter cast from silicone. Nine devices have been built with axially oriented electrodes (see Figure 13), two with regeneration tube electrode channels (see Figure 15), and one with a hybrid design incorporating both electrode configurations. All electrodes have been constructed using 2 mil Pt/Ir wire with 0.5 mil Teflon insulation.

Axial Wire Electrode Array with Closed-end Cuff

The initial stimulating electrode array design consisted of a closed-end silicone cuff with an array of axially-oriented Pt/Ir wire electrodes with 1 mm of deinsulated wire at the tip; this design is shown in Figure 13. As mentioned above, regeneration halted 1-2 mm proximal to the distal end of the nerve cuff, leaving a "plasma zone" at the distal end of the cuff.

Intraoperatively, a tube connected to the distal end of the cuff was used to apply a vacuum to the cuff to draw the nerve stump onto the electrodes during implantation. During post-mortem dissection of the one of the implanted nerves, a mass of axons was observed to have regenerated through this vacuum port. The remainder of axons had not significantly regenerated. The only significant presence of axons around the electrode array was comprised of the single population of axons which had regenerated through the hole in the silicone cuff.

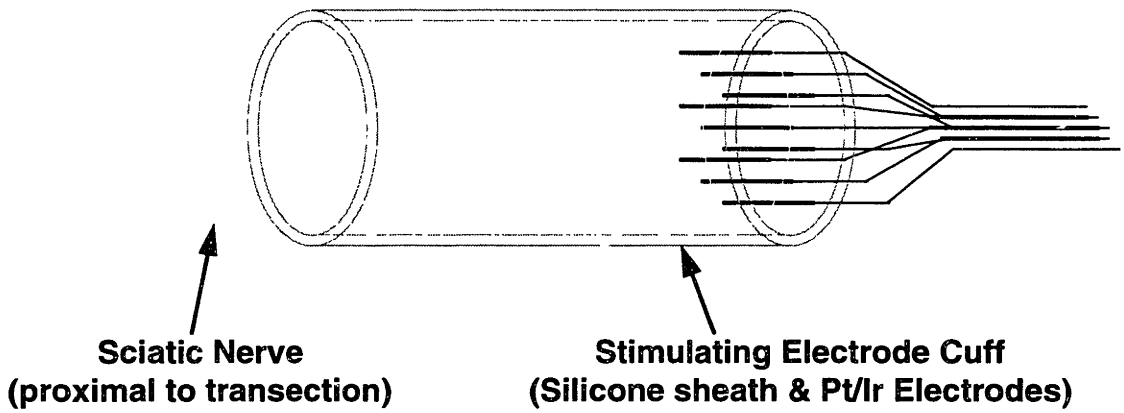

Figure 13: Axial Wire Electrode Array with Closed End Cuff

This motivated the inclusion of an array of regeneration holes located at the distal end of the nerve cuff. A circumferential array of regeneration ports, it was reasoned, may encourage regeneration of the transected axons through the entire volume of axially-oriented wire electrode array as discussed below.

Axial Wire Electrode Array with Regeneration Ports

The axial wire electrode array with regeneration ports is shown in Figure 14. An array of 8 to 12 regeneration ports measuring several hundred microns were spaced evenly along the circumference of the silicone nerve cuff at its distal end. Axonal regeneration was observed through the majority of these regeneration ports, and neuromas formed distal to the nerve cuff in several of the implanted animals.

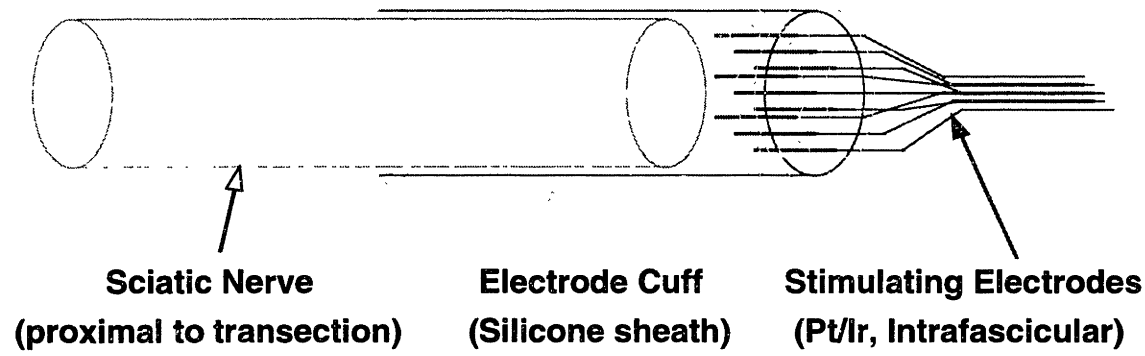

Figure 14: Axial Wire Electrode Array with Regeneration Ports

Successful evoked potential recordings from arrays of this design prompted the exploration of a regeneration tube design, shown below, which is expected to provide both a lower stimulation threshold and greater stimulation specificity.

Regeneration Tube Electrode Array with Enclosed Wire Electrodes

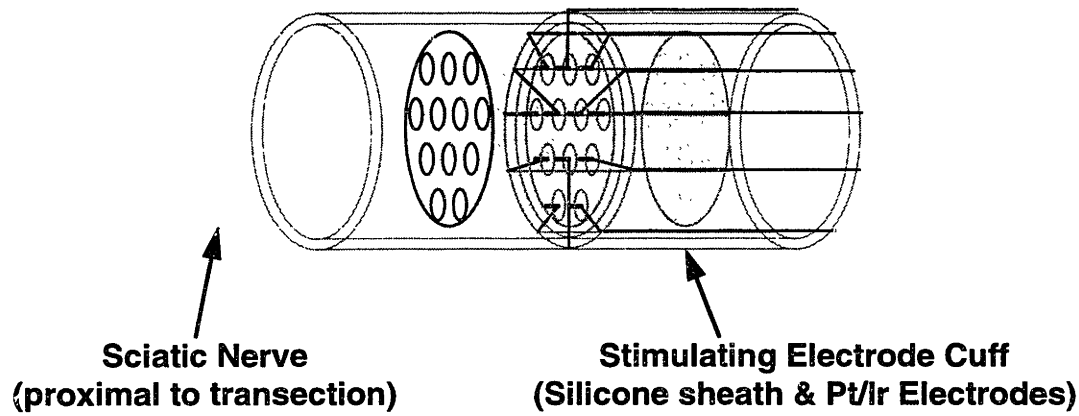

Figure 15: Regeneration Tube Electrode Array

The regeneration tube electrode array design shown in Figure 15 consists of an array of regeneration tubes, each containing a stimulating wire electrode. The nerve cuff or body of the implant is constructed from silicone tube. The regeneration tube array is cast from silicone, and electrodes are manually inserted and secured in place using uncured silicone. the entire regeneration tube array is secured within the nerve cuff using uncured silicone. The bundle of Pt/Ir wires is drawn through a silicone tube which serves as an outer insulating layer and mechanical strain relief. The proximal ends of the Pt/Ir wires are

soldered to the percutaneous plug using a silver-based solder. After soldering is complete, a larger gauge stainless steel wire is fastened between the implant body and the percutaneous plug. This wire courses within the outer insulating silicone tube and provides protection against mechanical tension on the Pt/Ir wires.

The length of the cylindrical regeneration tubes greatly exceed the diameter. this restricts the current from the electrode to flow axially, establishing an electrical potential gradient along the axon segment surrounded by the tube. Because of the large length to diameter ratio, the great majority of the electrical resistance is within the narrow regeneration tube, therefore, the electrical potential gradient outside the tube is negligible. As a result, axonal stimulation, which is induced by the electrical potential gradient, is restricted to the subpopulation contained within any given tube.

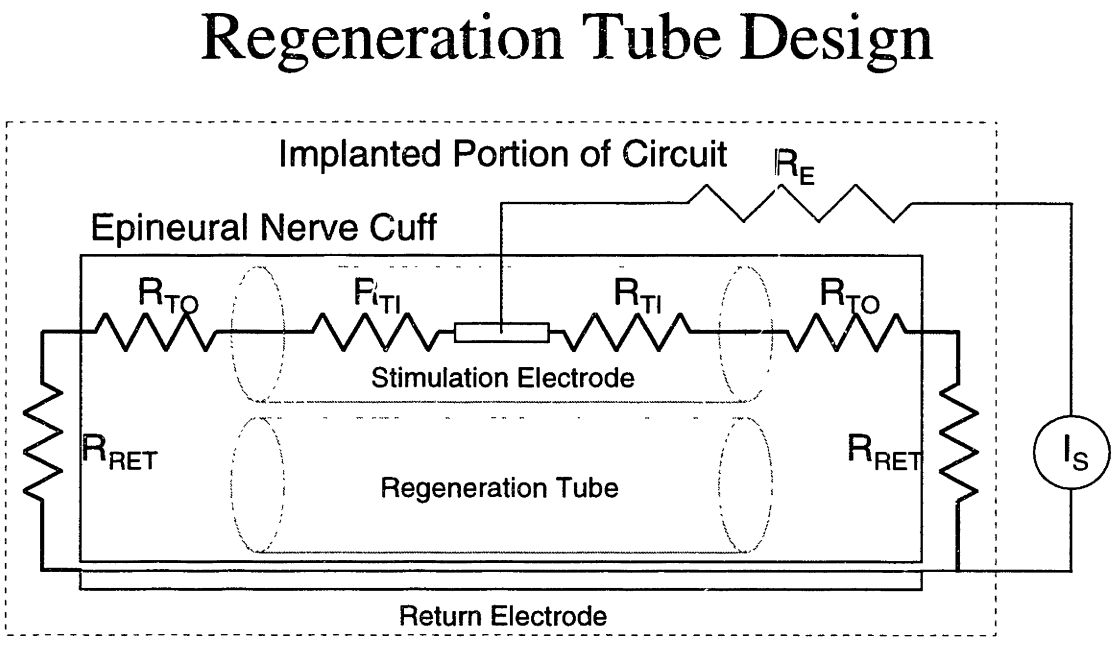

Figure 16: Regeneration Tube Electrode Array: Simplified Circuit Schematic

A simplified schematic representation of the regeneration tube design is given in Figure 16. Current flows from the stimulator circuitry through the electrode and its inherent resistance, through the extracellular fluid (ECF) in the narrow Regeneration Tubes (labeled R_{TI}, Inner Tube Resistance), through the ECF of the larger diameter of the Silicone Cuff (labeled R_{TO}, Outer Tube Resistance), and to the return electrode (labeled R_{RET}) on the outside of the cuff.

The Regeneration Tube impedance (R_{TI}), indicated within the tube, is several orders of magnitude higher than the impedance of the extracellular fluid in the larger silicone cuff and that along the current path to the return electrode

outside the cuff. This resistance, calculated from the regeneration tube geometry and published estimates of extracellular volume conductance [43, 44] ranges from 100 to 300 kilohms. Similarly, the calculated resistance of the nerve cuff tube or outer tube (R_{TO}) ranges from 5 to 10 kilohms.

Since R_{TI} is nearly 2 orders of magnitude greater than R_{TO}, virtually all of the electrical potential drop induced by the stimulation current is distributed as a linear gradient along the Regeneration Tube, causing depolarization along the Nodes of Ranvier contained within the tubes, most adjacent to the electrode. The electrical potential gradient induced along axons outside of a given regeneration tube is negligible compared to that within the tube, providing a potentially high degree of stimulation selectivity or minimal crosstalk between stimulation channels.

One evoked potential stimulation experiment conducted immediately postoperatively revealed a stimulation threshold on the order of 3 microamps, supporting the theoretical reasoning motivating this design. During the implantation procedure, axons are drawn into the regeneration tubes using a gentle vacuum applied to the distal end of the implanted array. Presumably these axons were stimulated in this experiment. Consistent with the expected axonal response to transection, these axons presumably later died back to the preceding Node of Ranvier. The high aspect ratios of the regeneration tubes (narrow diameters relative to lengths) appear to have impeded regeneration, as confirmed at necropsy. Consistent with these findings, chronic monitoring via neurophysiological and behavioral techniques failed to reproduce stimulation thresholds of this very low magnitude.

Results: Chronic Stimulating Neuroelectric Interface

Implant Evaluation: Histology of Regenerated Peripheral Nerve

Figure 17 depicts representative histology of regenerated nerve in a stimulating electrode array implant. Quantitative histological analysis, including axon histograms and axon densities is planned in the future.

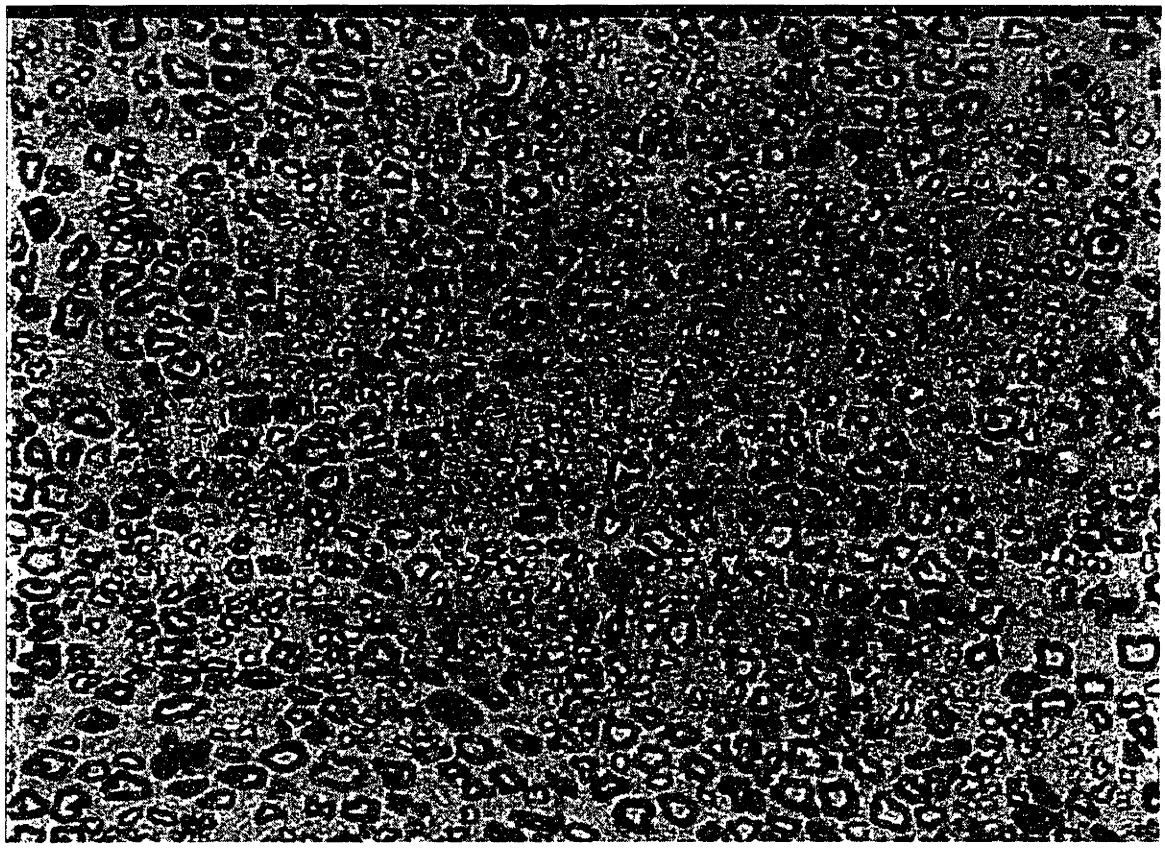

Figure 17: Histology: Regenerated Nerve in Stimulating Electrode Array (Rabbit AY)

Implant Evaluation using Evoked Potential Monitoring

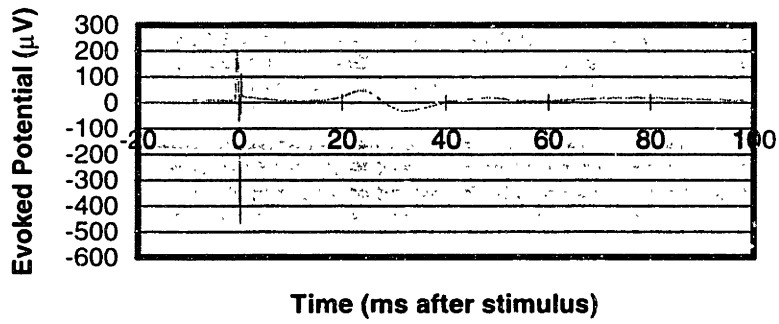

Figure 18: Cortical Evoked Potential Recording

Evoked potentials (EPs) have been recorded for as long as 129 days after implantation. The lowest individual electrode chronic stimulation threshold (as detectable by EP monitoring) has been found to be 35 microamps. One recording performed immediately post-operatively demonstrated a threshold of 15 microamps; this is believed to involve the stimulation of a nerve section drawn *into* one of the *regeneration* tubes during implantation. A typical somatosensory evoked potential is given in Figure 18. Note the large electrical stimulus artifact at t=0 milliseconds and the biphasic EP with an initial peak at t=24 milliseconds.

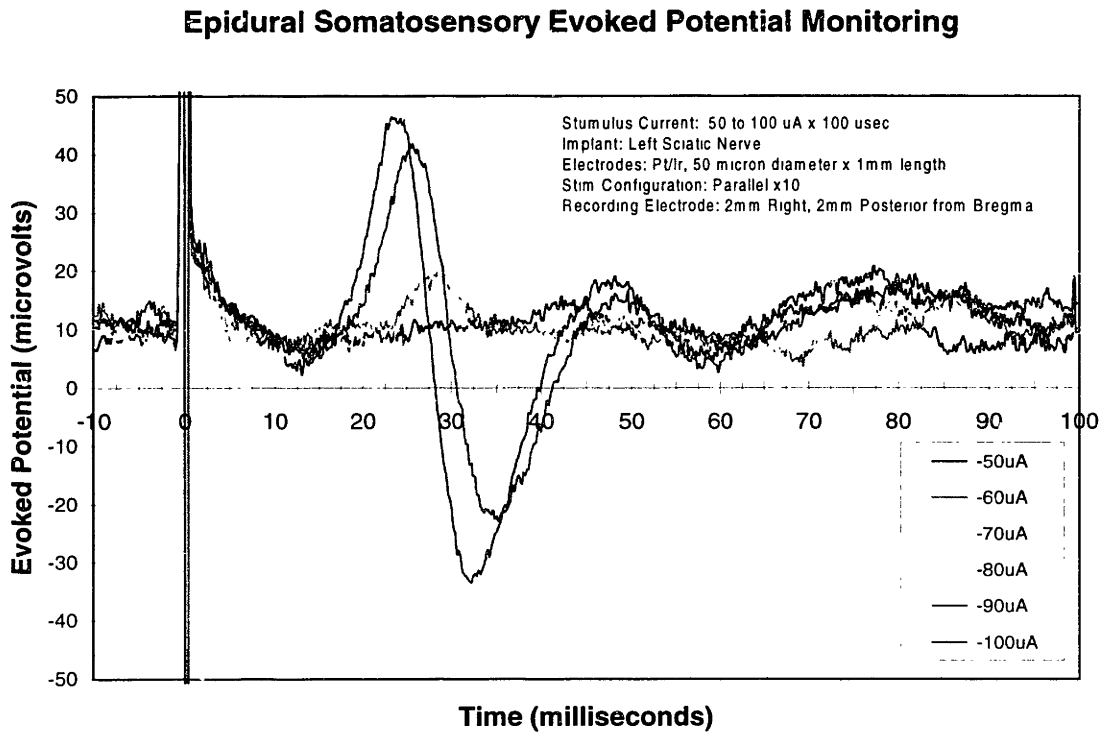

Figure 19: Somatosensory Evoked Potentials for Stimulation Current Range (Rabbit AY)

Figure 19 shows the somatosensory evoked potential (SEP) elicited by a range of stimulation currents. Within the range shown, SEP amplitude varies approximately monotonically with stimulation current amplitude. The stimulation threshold is better appreciated in Figure 20 in which the somatosensory evoked potential amplitudes are plotted as a function of electrical stimulation current.

The rising edge of the SEP waveform, seen clearly at higher stimulation amplitudes, is found to occur at 18 milliseconds following stimulation. The neural distance traversed from the implant to the brainstem is approximately 30 centimeters. Neglecting brainstem and cortical conduction and synaptic delay, this would correspond to a conduction velocity of approximately 30 centimeters / 18 milliseconds = 17 meters per second, which is consistent with expected conduction velocities. At lower stimulation amplitudes, the SEP peak is noted to occur approximately 5 milliseconds later (28 versus 23 milliseconds following the stimulus). Perhaps in these lower amplitude waveforms, the more distal and amplified cortical activity in higher centers is being observed, and the activity in the more proximal and less amplified primary motor cortex may only be detected at higher stimulation levels.

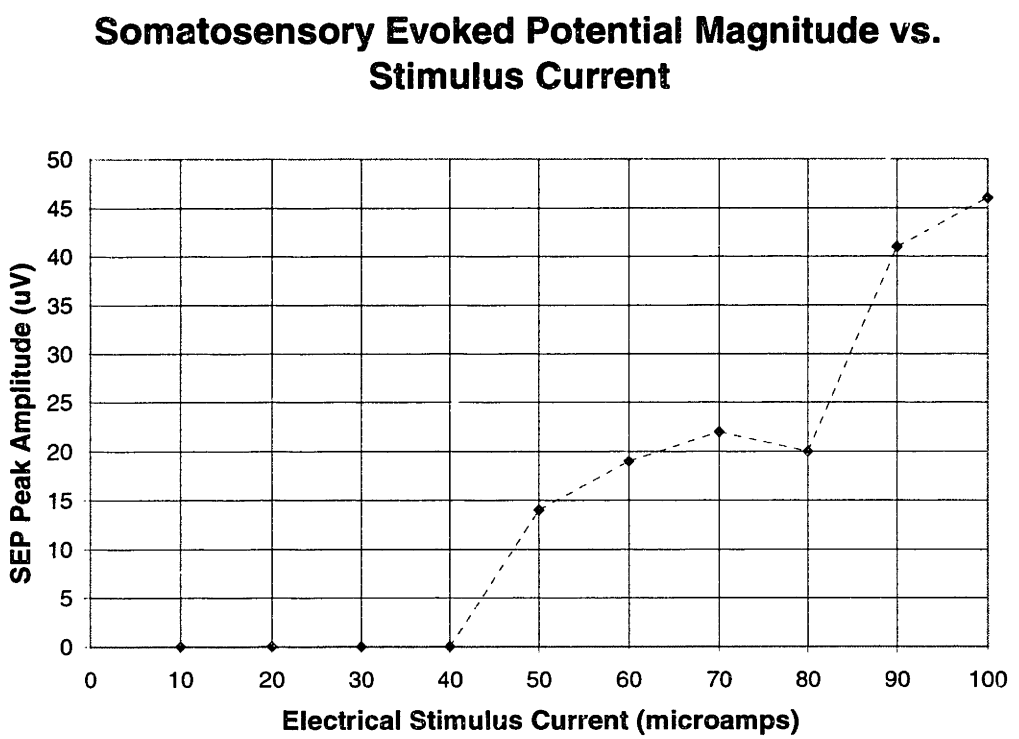

Figure 20: Somatosensory Evoked Potentials: Stimulation Threshold (Rabbit AY)

Implant Evaluation using Behavioral Conditioning and Monitoring

Classical conditioning of the eyeblink reflex conditioned stimuli has been reported in animal models [45, 46]. A conditioning technique in which the conditioned stimulus is the electrical stimulation of the sciatic nerve was developed.

In a series of behavioral conditioning experiments, the rabbits were trained to associate a conditioned electrical stimulus with an unconditioned corneal airpuff stimulus (which elicited the unconditioned eyeblink response). Many of the rabbits trained mad the association during the fourth consecutive day of training. Training days included typically one session of 50 eyeblink trials. By this behavioral testing, perception of electrical stimuli was demonstrated 118 days after implantation.

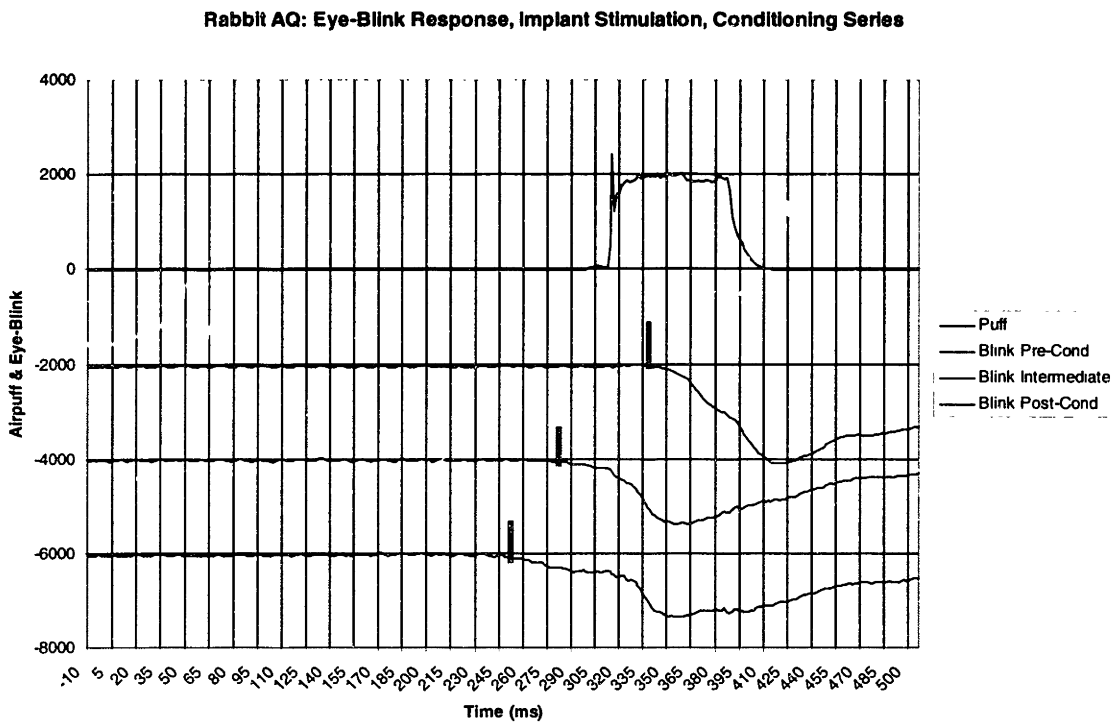

Figure 21: Eye-Blink Behavioral Conditioning, Implant Stimulation: Eye-Blink Advancement

Training of the Ax series rabbits was performed entirely using electrical stimuli delivered to the implanted sciatic nerve, as shown in Figure 21. Training of later rabbits, the Bx series, was performed using electrical stimuli delivered via gel electrodes to the skin corresponding to the region of the leg subserved by the sciatic nerve. This surface stimulation produced a small twitch of the skin, enabling visual verification by the author that a stimulus was being delivered and perceived by the animal. This was particularly useful because the perception thresholds of the implanted electrode array are unknown initially, and there is a risk of damage to the implanted nerve if stimuli are delivered at unnecessarily

high amplitudes during training. This allowed training to be performed at a moderate stimulus intensity without risk to the nerve. Once conditioning is achieved, only a small series of stimuli, delivered with gradually increasing amplitudes, is required to verify perception of stimuli from the implanted electrode array.

Eye-Blink advancement is demonstrated in Figure 21 in which the top curve represents the airpuff pressure measured near the eye, and the successively lower three curves demonstrate progressively advancing eye-blink response to the electrical stimulus delivered at t=0 milliseconds. (Vertical axis units are normalized, and the waveforms are offset on the vertical axis for clarity.) The vertical bars on these figures (Figure 21 to Figure 26) indicate the onset of the eyeblink; the second negative phase is a more vigorous portion of the blink which occurs in response to the airpuff stimulus.

Figure 22 shows the eye-blink response at the beginning of the training regimen. The upper trace represents the electrical stimulus delivered to the stimulating electrode array implanted on the left sciatic nerve. The middle trace represents the airpuff pressure, sensed by a pressure transducer connected to the silicone nozzle which is held approximately 1 cm from the left cornea of the rabbit. The lower trace is the infrared (IR) reflectance sensed by an IR emitter detector pair mounted adjacent to the silicone airpuff nozzle. Reflectance changes as the nicotinic membrane advances over the eye and the as the eyelid closes, indicating the occurrence of an eyeblink. The electrical stimulus onset, airpuff pressure onset, and eyeblink onset are shown at t=15 milliseconds, 265 milliseconds, and 305 milliseconds, respectively. Thus, the eyeblink follows the electrical stimulus and airpuff by 290 and 40 milliseconds, respectively.

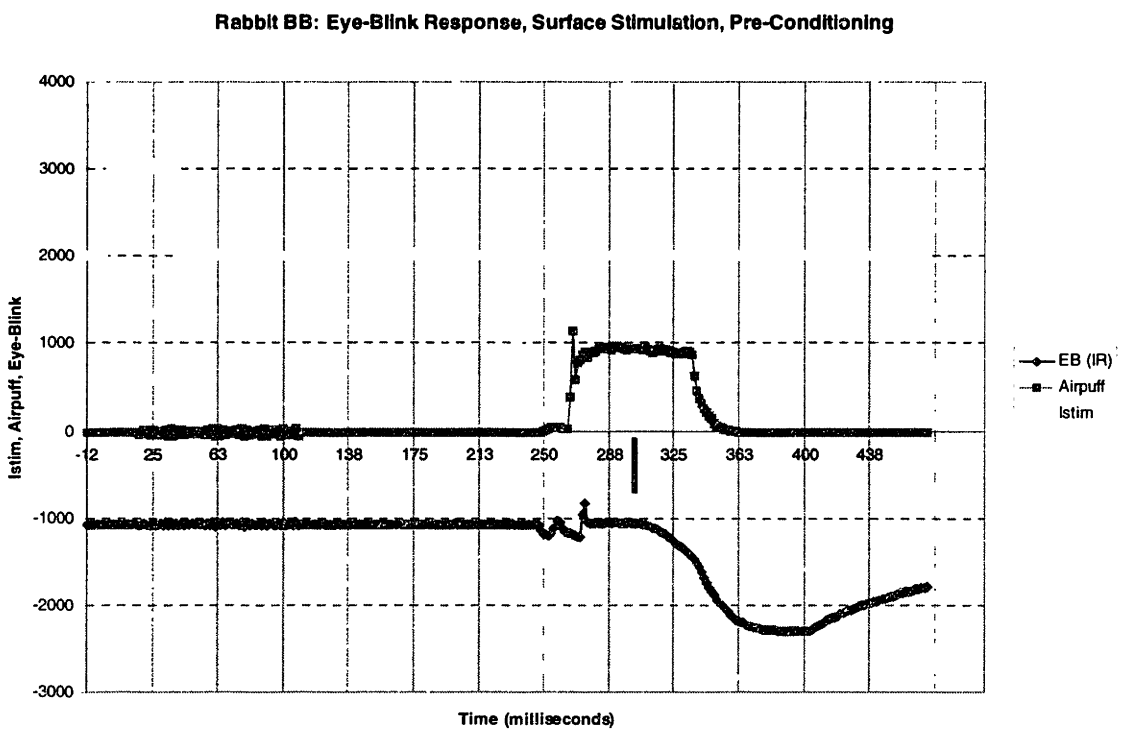

Figure 22: Eye-Blink Response, Surface Stimulation, Pre-Conditioning

In Figure 23, the eyeblink response in the same rabbit later in training is shown. The electrical stimulus onset, airpuff pressure onset, and eyeblink onset are shown at t=15 milliseconds, 265 milliseconds, and 285 milliseconds, respectively. Thus, the eyeblink follows the electrical stimulus and airpuff by 270 and 20 milliseconds, respectively. Note the advancement in time of the onset of the eyeblink (lower) waveform, by 20 milliseconds relative to the untrained state.

In Figure 24, eyeblink conditioning of Rabbit BB in the fully trained state is shown. The electrical stimulus onset, airpuff pressure onset, and eyeblink onset are shown at t=15 milliseconds, 265 milliseconds, and 120 milliseconds, respectively. Thus, the eyeblink follows the electrical stimulus by 105 milliseconds and *precedes* the airpuff by 145 milliseconds. Note the advancement in time of the onset of the eyeblink (lower) waveform, by 185 milliseconds relative to the untrained state.

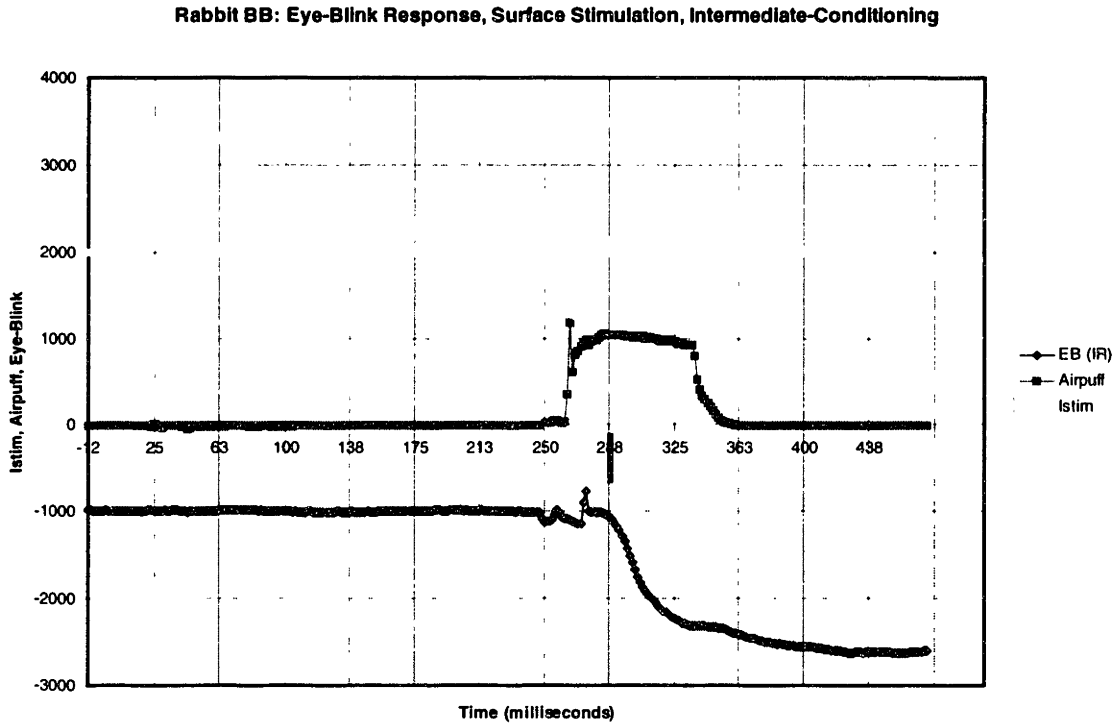

Figure 23: Eye-Blink Response, Surface Stimulation, Intermediate-Conditioning

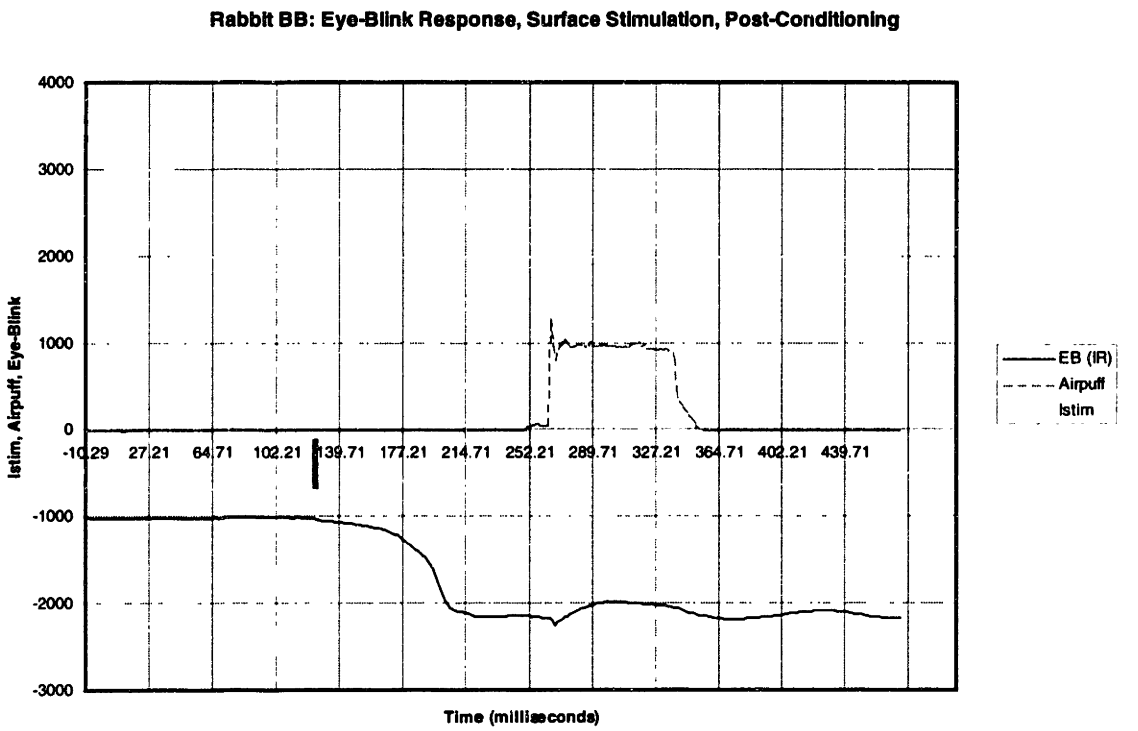

Figure 24: Eye-Blink Response, Surface Stimulation, Post-Conditioning

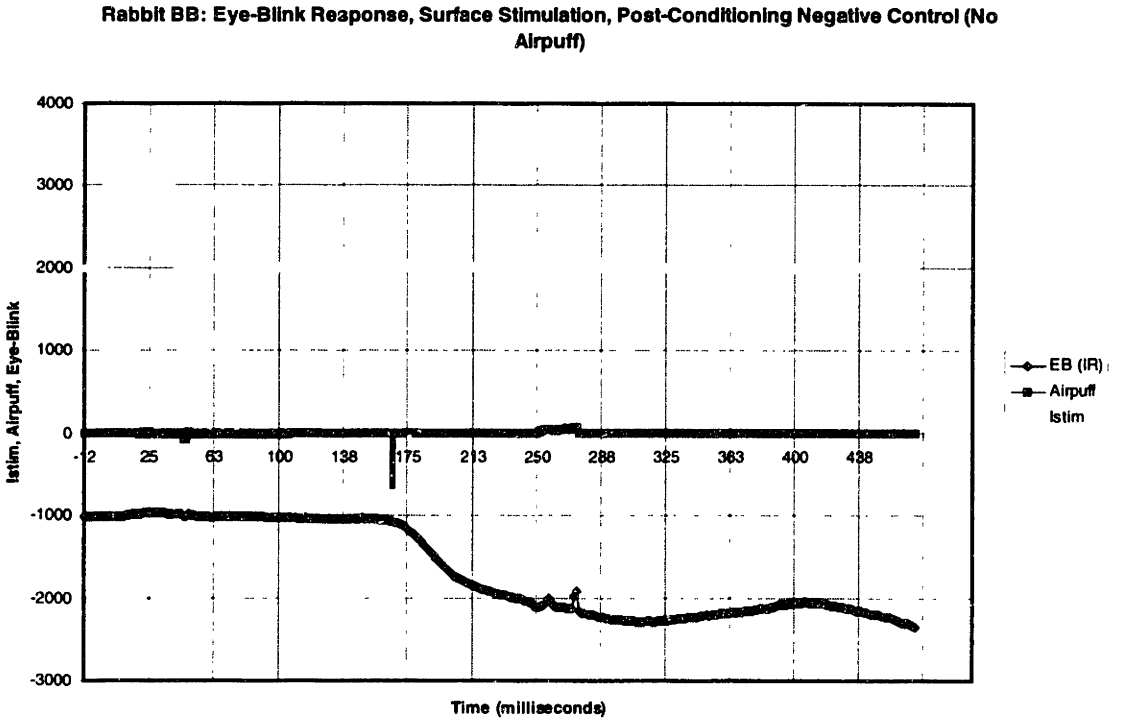

Figure 25: Eye-Blink Response, Surface Stimulation, Post-Conditioning Negative Control (No Airpuff)

In Figure 25, a control for eyeblink conditioning of Rabbit BB in the fully trained state is shown. In this trial, no airpuff is delivered. The air pressure source was turned off in this trial; the very small signal present on the pressure waveform is an artifact resulting from electrical coupling of the pressure solenoid drive signal with the pressure sensor. The electrical stimulus onset and eyeblink onset are shown at t=15 milliseconds and 160 milliseconds, respectively. Thus, the eyeblink follows the electrical stimulus by 145 milliseconds, similar to the fully trained trial depicted in Figure 24.

After successful conditioning was achieved using surface stimulation of the leg, as shown in 25, stimulation of the implanted sciatic nerve was performed. Usually within the early portion of the first session, i.e. by approximately 10 trials, the rabbit made the association with the new implanted stimulus, and the post-conditioned response to the implanted stimulus was obtained. This post-conditioned response to implant stimulation is shown in Figure 26

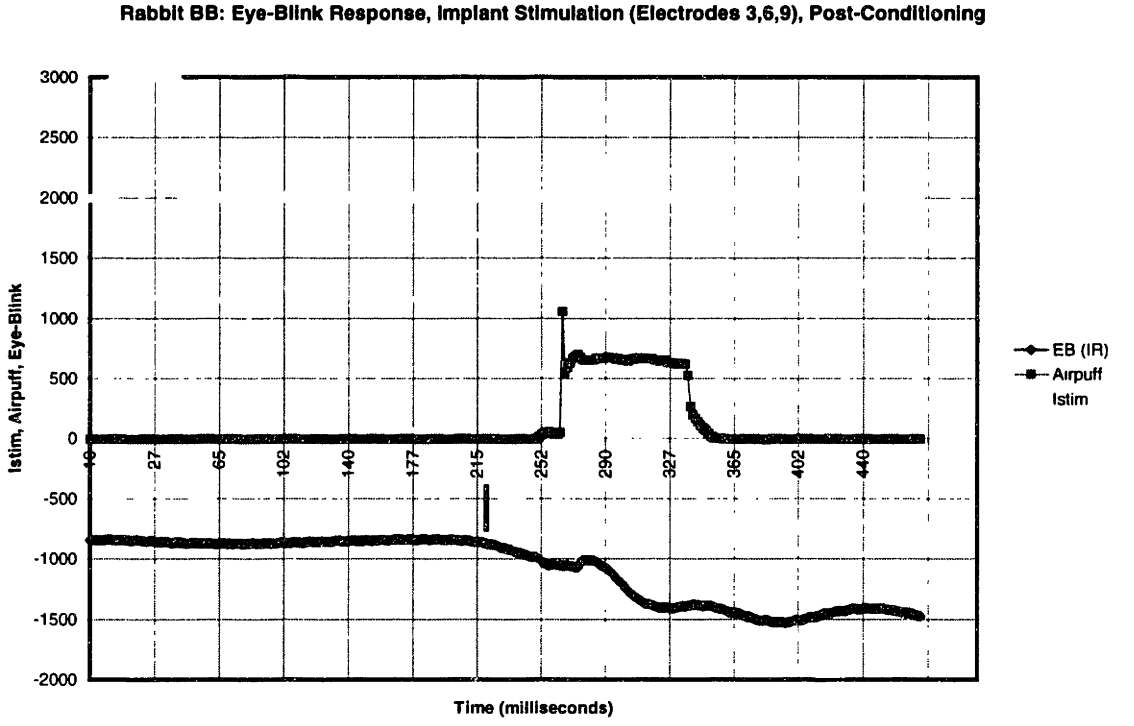

Figure 26: Eye-Blink Response, Implant Stimulation, Post Conditioning

Implant Evaluation: Electrode Impedance Monitoring

Electrical impedance of the implanted stimulating electrodes was monitored. Measurement consisted of sequentially measuring the individual impedances of each stimulating electrode relative to the common return electrode or relative to a gel electrode mounted on the ipsilateral ear. A 1 kilohertz sinusoidal signal was delivered separately to each of the stimulating electrodes and the resulting current waveform was sampled. The amplitude and phase of the current waveform was calculated relative to the voltage waveform. From the amplitude ratio and phase shift, the magnitude and phase of the electrode impedances is calculated.

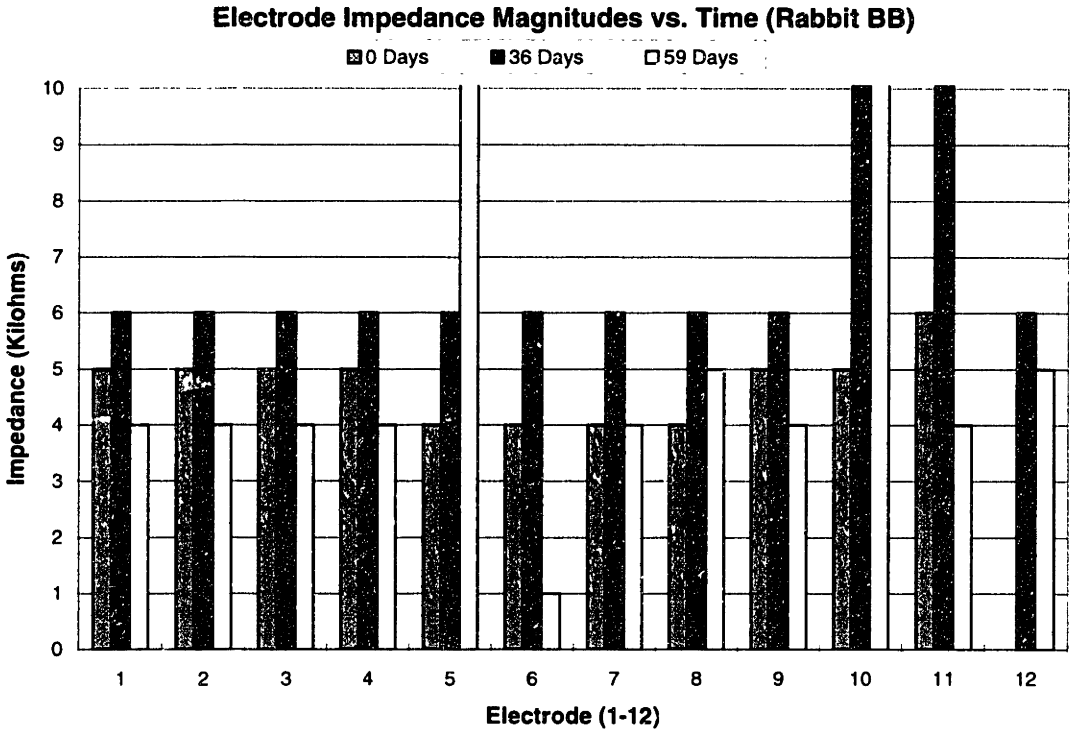

Figure 27: Electrode Characterization: Impedance Magnitude vs. Time

Figure 27 shows the electrode impedance magnitudes for the 12 stimulating electrodes followed for 59 days post implantation. The impedances of 9 of the 12 electrodes are seen to be relatively stable. Impedance amplitudes of 2 electrodes increase to several hundred kilohms by day 36 indicating electrode fracture, and that of one electrode increases to nearly 70 kilohms by day 59, also potentially indicating fracture or other compromise.

Nerve Regeneration Tube Array: Study Results

In parallel with the design of the regeneration tube electrode array, a pilot nerve regeneration study was performed to assess the axonal regenerative capacity through non-wired "blank" silicone tubes. The original design consisted of an array of Dow-Corning Silastic (MDX-4210) tubes (0.012" inner dia.). Due to the unavailability of Dow-Corning silicone products for medical implantation, evaluation of alternative medical-grade silicone sources was conducted. Because of concerns regarding surface purity of commercially available medical-grade extruded silicone tubing, a tube casting technique was developed. In this study, silicone arrays of varying lengths (1, 2, 5, and 10 mm) were cast using NuSil Technology medical-grade silicone types MED-4211 and MED-6210. The implants consisted of twelve regeneration tubes of 0.012" inside diameter, the cross section of which is shown in Figure 28.

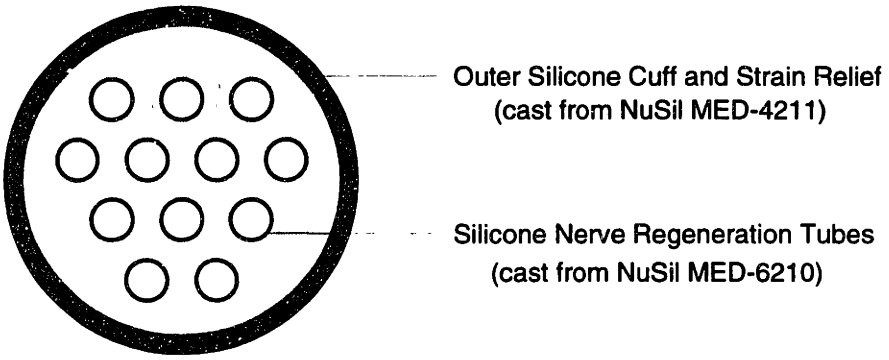

Figure 28: Cast Non-Wired Regeneration Tube Array

Neural regeneration was observed through the 1 mm length implant, but no appreciable regeneration was found in the implants of 2, 5, and 10 mm, respectively. Further investigation will be necessary to determine optimal geometries for a regeneration tube electrode array.

Discussion of Chronic Stimulating Neuroelectric Interface

Evoked potential monitoring has demonstrated implant functionality for up to 129 days, and concurrent behavioral conditioning has established functionality for 118 days. The more recently implemented behavioral conditioning has shown promise as a more sensitive means of monitoring implant functionality. Further tests are required to determine the sensitivity of the behavioral conditioning technique and to explore the possibility of behavioral conditioning as a means to discriminate among multiple channel stimulation.

Discussion of Objectives

Several designs for multichannel microelectrode interfaces were explored. Success was greatest with the design which provided the least obstruction to neural regeneration, i.e. the axial wire microelectrode array design. Although the regeneration tube design possessed several theoretical advantages over the axial wire design, difficulty in achieving satisfactory regeneration limited its performance. The passive regeneration tube study suggested that with sufficiently short regeneration tubes, that design may prove functional. Similarly, exploration of regeneration tubes of larger diameter may prove fruitful. Further optimization of regeneration tube geometry, augmented with regeneration enhancing agents including laminin coatings and nerve growth factors, appears to be a next logical avenue of investigation.

By maintaining many hundred microns of space between the silicone nerve cuff and the electrode surfaces, detrimental effects on electrode

performance of fibrosis and encapsulation of the silicone were minimized. Consistent with prior literature, the inert platinum-iridium wires proved resistant to the chemical environment of the body and did not elicit an immunological response.

This research demonstrated the chronic viability of sensory axons for a duration of 129 days following nerve transection. This confirms preservation of at least some portion of nerve functionality despite the absence of a distal nerve stump or sensory organs. Further quantitative histological analysis will be required to assess axon diameter changes.

Relative stability of the impedances of nonfractured electrodes was . Long-term in-vivo electrode impedance monitoring revealed Over the course of this investigation, as various strain and tension relief techniques were incorporated into the design, the incidence of electrode fracture decreased. Continued research in failure mode analysis and reduction should prove fruitful to the development of a chronically functional implant.

Sensory perception thresholds were found to be on the order of 30-60 microamps and were of the same order of magnitude as those determined by somatosensory evoked potential monitoring.

Discussion and Future Recommendations for Implant Design

Maintenance of open paths for axonal regeneration appear to be important to achieve a functional interface. Regeneration halted several millimeters short of the distal end of a closed nerve cuff.

Regeneration tube electrode arrays appear to hold promise in reducing stimulation thresholds and delivering channel selectivity; however, further development remains to achieve satisfactory regeneration. Future routes of investigation include further geometric optimization as well as evaluation of surface coatings and trophic factors. Prior animal studies provide evidence that laminin enhances axonal regeneration [47, 48]. Given the limited regeneration observed in the regeneration tube electrode array designs, investigation of laminin enhanced designs would appear to be one germane next step in the development of this theoretically promising design.

References

1. Clippinger, F.W., *A sensory feedback system for an upper-limb amputation prosthesis.* Bulletin of Prosthetics Research, 1974. **BPR 10-22**: p. 247-258.
2. Clippinger, F.W., in *Textbook of Surgery: The Biological Basis of Modern Surgical Practice*, D.C.e. Sabiston, Editor. 1977, W.B. Saunders: Philadelphia. p. pp. 1582-1594.
3. Clippinger, F.W., *et al.*, *Afferent sensory feedback for lower extremity prosthesis.* Clinical Orthopaedics and Related Research, 1982. **169**: p. 202-206.
4. Edell, D.J., *Development of a chronic neuroelectronic interface*, . 1980, U.C. Davis.
5. Kovacs, G.T., C.W. Storment, and J.M. Rosen, *Regeneration microelectrode array for peripheral nerve recording and stimulation.* IEEE Transactions on Biomedical Engineering, 1992. **39**(9): p. 893-902.
6. Canby, E.T., *A History of Electricity.* 1962, New York: Hawthorne Books. p. 21.
7. Frey, v.M., *Physiological experiments on the vibratory sensation (German).* Z. Biol., 1915. **65**: p. 417-427.
8. Adrian, E.D., *The response of human sensory nerves to currents of short duration.* Journal of Physiology (London), 1919. **53**: p. 70-85.
9. Beeker, T.W., J. During, and A. Den Hertog, *Technical note: Artificial touch in a hand prosthesis.* Medical & Biological Engineering, 1967. **5**: p. 47-49.
10. Schmidl, H., *The importance of information feedback in prostheses for the upper limbs.* Prosthetics and Orthotics International, 1977. **1**: p. 21-24.
11. Shannon, G.F., *A myoelectrically-controlled prosthesis with sensory feedback.* Medical & Biological Engineering & Computing, 1979. **17**: p. 73-80.
12. Prior, R.E., *et al.*, *Supplemental sensory feedback for the VA/NU myoelectric hand: Background and feasibility.* Bulletin of Prosthetics Research, 1976. **10-26**: p. 170-190.
13. Scott, R.N., *et al.*, *Sensory feedback system compatible with myoelectric control.* Medical & Biological Engineering & Computing, 1980. **18**: p. 65-69.
14. Szeto, A.Y.J., *Comparison of codes for sensory feedback using electrocutaneous tracking.* Annals of Biomedical Engineering, 1977. **5**: p. 367-383.
15. Kaczmarek, K.A., *et al.*, *Electrotactile and vibrotactile displays for sensory substitution.* IEEE Transactions on Biomedical Engineering, 1991. **38**: p. 1-16.
16. Szeto, A.Y.J. and F.A. Saunders, *Electrocutaneous stimulation for sensory communication in rehabilitation engineering.* IEEE Transactions on Biomedical Engineering, 1982. **BME-29**(4): p. 300-308.

17. Szeto, A.Y.J. and R.R. Riso, *Sensory feedback using electrical stimulation of the tactile sense*, in *Rehabilitation Engineering*, R.G. Smith and J. Lesley, Editors. 1990, Chemical Rubber Company (CRC) Press: Boca Raton, FL. p. pp. 29-78.
18. Phillips, C.A., *Sensory feedback control of upper- and lower-extremity motor prostheses.* CRC Crit Rev Biomed Eng, 1988. **16**: p. 105-140.
19. Shannon, G.F., *A comparison of alternative means of providing sensory feedback on upper limb prostheses.* Medical and Biological Engineering, 1976. **14**: p. 289-294.
20. Lovely, D.F., B.S. Hudgins, and R.N. Scott, *Technical note: Implantable myoelectric control system with sensory feedback.* Medical & Biological Engineering & Computing, 1985. **23**: p. 87-89.
21. White, J.C. and W.H. Sweet, *Pain and the Neurosurgeon: A Forty Year Experience*. 1969, Springfield, Ill: Charles C. Thomas. 895-896.
22. Nashold, B.S., Jr., J.B. Mullen, and R. Avery, *Peripheral nerve stimulation for pain relief using a multicontact electrode system.* Journal of Neurosurgery, 1979. **51**: p. 872-873.
23. Nashold, B.S.J., *et al.*, *Long-term pain control by direct peripheral-nerve stimulation.* Journal of Bone and Joint Surgery, 1982. **64-A**(1): p. 1-10.
24. Fields, R.D., *et al.*, *Nerve regeneration through artificial tubular implants.* Progress in Neurobiology, 1989. **33**: p. 87-134.
25. Lundborg, G., *et al.*, *Nerve regeneration in silicone chambers: Influence of gap length and of distal stump components.* Experimental Neurology, 1982. **76**: p. 361-375.
26. Scaravilli, F., *The influence of distal environment on peripheral nerve regeneration across a gap.* Journal of Neurocytology, 1984. **13**: p. 1027-1041.
27. Gutmann, E. and F. Sanders, *Recovery of fibre numbers and diameters in the regeneration of peripheral nerves.* Journal of Physiology, 1943. **101**: p. 489-518.
28. Weiss, P., M. Edds, and M. Cavanaugh, *The effect of terminal connections on the caliber of nerve fibers.* Anat. Rec., 1945. **92**: p. 215-233.
29. Aitken, J., M. Sharman, and J. Young, *Maturation of regenerating nerve fibers with various peripheral connexions.* A. Anat. (Lond.), 1947. **81**: p. 1-22.
30. Aitken, J. and P. Thomas, *Retrograde changes in fibre size following nerve section.* J. Anat. (Lond.), 1962. **96**: p. 121-129.
31. Cragg, B. and P. Thomas, *Changes in conduction velocity and fibre size proximal to peripheral nerve lesions.* J. Physiol., 1961. **157**: p. 315-327.
32. Hoffer, J.A., R.B. Stein, and T. Gordon, *Differential atrophy of sensory and motor fibers following section of cat peripheral nerves.* Brain Research, 1979. **178**: p. 347-361.
33. Marks, A., *Bullfrog nerve regeneration into porous implant.* Anatomical Record, 1969. **163**: p. 226.

34. Mannard, A., R. Stein, and D. Charles, *Regeneration electrode units: implants for recording from single peripheral nerve fibers in freely moving animals.* Science, 1974. **183**(124): p. 547-549.
35. Stein, R., *et al., Principles underlying new methods for chronic neural recording.* Canadian Journal of Neurological Sciences, 1975. **2**(2): p. 235-244.
36. Loeb, G., W. Marks, and P. Beatty, *Analysis and microelectronic design of tubular electrode arrays intended for chronic, multiple single unit recordings from captured nerve fibers.* Medical & Biological Engineering & Computing, 1977. **15**(2): p. 195-201.
37. Sunderland, S., *Nerves and Nerve Injuries.* 2nd ed. ed. 1978, New York: Churchill-Livingstone.
38. Edell, D., J. Churchill, and I. Gourley, *Biocompatibility of a silicon based peripheral nerve electrode.* Biomaterials, Medical Devices & Artificial Organs, 1982. **10**(2): p. 103-122.
39. Edell, D., *A peripheral nerve information transducer for amputees: long-term multichannel recordings from rabbit peripheral nerves.* IEEE Transactions on biomedical Engineering, 1986. **33**(2): p. 203-214.
40. Woolsey, C.N. and D. Fairman, *Contralateral, ipsilateral, and bilateral representation of cutaneous receptors in somatic areas I and II of the cerebral cortex of pig, sheep, and other animals.* Surgery, 1946. **19**: p. 684-702.
41. DiLorenzo, D.J. and D.J. Edell, *Acute Somatosensory Cortical Mapping of Sciatic Nerve Stimulation (unpublished results).* 1994.
42. Gould, H.J., *Body surface maps in the somatosensory cortex of rabbit.* The Journal of Comparative Neurology, 1986. **243**: p. 207-233.
43. Trayanova, N., C.S. Henriquez, and R. Plonsey, *Extracellular potentials and currents of a single active fiber in a restricted volume conductor.* Annals of Biomedical Engineering, 1990. **18**(3): p. 219-238.
44. Cartee, L.A. and R. Plonsey, *The transient subthreshold response of spherical and cylindrical cell models to extracellular stimulation.* IEEE Transactions on Biomedical Engineering, 1992. **39**(1): p. 76-85.
45. Buchanan, S., *Differential and reversal Pavlovian conditioning in rabbits with mediodorsal thalamic lesions: assessment of heart rate and eyeblink responses.* Experimental Brain Research, 1991. **86**(1): p. 174-81.
46. Irwin, K., *et al., Distribution of c-fos expression in brainstem neurons associated with conditioning and pseudo-conditioning of the rabbit nictitating membrane reflex.* Neuroscience Letters, 1992. **148**(1-2): p. 71-75.
47. Navarro, X., *et al., Effects of laminin on functional reinnervation of target organs by regenerating axons.* Neuroreport, 1991. **2**(1): p. 37-40.
48. Nakao, Y., *An experimental study on the effect of laminin in vivo on promoting regeneration of axons [Japanese].* Nippon Seikeigeka Gakkai Zasshi - Journal of the Japanese Orthopaedic Association, 1992. **66**(4): p. 334-349.

THESIS PROCESSING SLIP

FIXED FIELD: ill. _____ name _____

index _____ biblio _____

▶ COPIES: (Archives) Aero Dewey Eng Hum

Lindgren Music Rotch Science (Schwarzman)

TITLE VARIES: ▶ ☐ _____

NAME VARIES: ▶ ☑ John _____

IMPRINT: (COPYRIGHT) _____

▶ COLLATION: 44 l

▶ ADD: DEGREE: _____ ▶ DEPT.: _____

SUPERVISORS: _____

NOTES:

cat'r: date:

page: 3112.177 212

▶ DEPT: HST

▶ YEAR: 1999 ▶ DEGREE: S.M.

▶ NAME: DILORENZO, [illegible]